



Appendix L. Commercial Data in NASA Conjunction Assessment

The breadth and quality of commercial SSA data has developed in the last decade from essentially no commercial presence at all to the presence of a number of different vendors, each specializing individually in radar, optical, or passive radio frequency satellite tracking. In addition to tracking measurement data, vendor offerings now include additional SSA products such as vectors, ephemerides, and even conjunction risk assessment analysis outputs such as Conjunction Data Messages (CDMs).

In examining and facilitating the use of commercial data in NASA conjunction risk assessment calculations, CARA and JSC FOD adhere to the following principles:

1. Use raw observation (measurement) data only and combine with Space Surveillance Network (SSN) observations for a single solution
2. Validate all non-SSN data
3. Undertake a cost/benefit analysis before purchasing commercial SSA data

More details on these principles are described below.

L.1 Use raw observation (measurement) data only and combine with SSN observations for a single solution

Of all the data types offered by commercial providers, only the raw satellite tracking data are at present fully and unambiguously of use to the NASA conjunction assessment enterprise.

Because NASA has access to both the USSPACECOM satellite tracking data from the SSN and the USSPACECOM space catalog maintenance operational system, NASA has the ability to include raw commercial observation data along with SSN tracking data into a combined close approach prediction. This process involves combining all of the measurement data on an object of interest from both the SSN and commercial sources to perform a single orbit determination. The predicted close approaches can then be calculated from this combined source. The CARA and JSC FOD personnel who are embedded in the 18 SDS work center at VSFB presently have this capability in a “sandbox” area on the operational system that is not used for routine operations. The sandbox area enables CARA/JSC FOD operators to combine the SSN and commercial data in a native and compatible way to produce a single risk assessment solution that can be acted upon unambiguously.

Work is also progressing on a regularization of the reception of commercial data into the 18 SDS enterprise; when such a capability is in place, conjunction assessment products deriving from combined commercial and DOD tracking data will be possible routinely. But receiving higher-level products from commercial vendors, such as vectors or even conjunction assessment outputs like CDMs, introduces multiple solutions into the enterprise and creates significant operational difficulties in trying to adjudicate among them.



Event evaluation in the presence of multiple solutions

There is presently a debate within the industry regarding the best way to proceed with event evaluation in the presence of multiple solutions. CARA/JSC FOD encounters a version of this situation in miniature each day in that most conjunction events possess two solutions: one that uses the DOD predicted position for the primary object state and a second that uses the O/O predicted ephemeris for that state. Counterintuitively, it is not always clear which of these two sources for the primary object predicted state is superior.

O/Os typically have more and better past position data on their satellite, either from telemetry tracking or onboard GPS fixes, and they also understand the configuration of their satellite better and thus should be able to calculate the components of the ballistic coefficient with more precision. The O/Os should then be able to come up with a better epoch solution on which to base prediction, and they are positioned to do a better job in prediction as well because they potentially possess a superior ballistic coefficient. However, O/O orbit determination software atmospheric density models often introduce more error into predicted states than the model used by the 18 SDS.

In the situation that CARA faces, the choice of a preferred data source is thus not straightforward because a number of factors influence the selection: the capabilities of the O/O's orbit determination software, the particular orbit that the satellite occupies, the degree to which the space weather situation is perturbed, and the span from the present time to TCA, among others.

Establishing a rubric of precedence

To reliably choose between these two information sources, CARA has performed a Verification and Validation (V&V) activity of the orbit determination products for selected NASA O/Os and has developed rubrics for selecting a particular solution (DOD- or O/O-based) source in particular contexts. A V&V activity of this type requires several months' worth of data and is complicated to perform, necessitating specialized tools and subject matter expert interpretation of the results. With multiple providers of information for both the primary and secondary objects involved in a conjunction, the situation would be that much more complicated.

Assimilative solution selection

An alternative to establishing a rubric of precedence for the multi-solution situation is using an assimilative modeling approach similar to that used for hurricane modeling.

The results from multiple providers are collected and comparatively analyzed, both visually and with formal clustering algorithms. Due to the large representation among the submissions (i.e., most of the individual results clustering around a single result), the hope is to be able to establish a supermajority result that suggests itself as the favored solution. Although such a procedure appears attractive at first, it encounters difficulties in implementation.

- First, it requires a sufficient number of providers supplying solutions to obtain meaningful data clusters. Clustering among, say, ten submitted solutions has the propensity to identify meaningful clusters and thus enable the drawing of certain



conclusions. With only two or three providers, this is not really possible. At present, the number of different providers is too small to use a clustering approach.

- Second, because of explainable and therefore expected discontinuities in space surveillance data sets, it is not unusual for minority submissions to an assimilative framework to represent the superior solution. The common situation of satellite maneuvers is a good example: only one of a set of providers may have detected a maneuver for one of the spacecraft in a conjunction and updated that spacecraft's state appropriately. This solution is clearly superior to other submissions that did not obtain tracking in time to identify the maneuver and correct the trajectory. But as a single solution representing this modified state, this solution will appear assimilatively as an outlier and is likely to be rejected. This scenario has played out repeatedly at the Sprint Advanced Concept Training (SAC-T) exercises conducted by the U.S. Space Force's Joint Commercial Operations (JCO) cell: a single vendor's submission differs appreciably from the other submissions yet is shown later to be the preferred solution.

In short, while assimilative solution selection remains a potentially helpful construct for employing multiple solutions contemporaneously to guide a single operational decision, more research and refinement are required before such a paradigm can be employed in an operationally satisfactory manner to support conjunction risk assessment.

Direct fusion of orbital solutions

Finally, there are proposals in the academic literature for the direct fusion of different orbital solutions, including CDMs from different providers, into a single solution that in principle combines the information of all the individual submissions.

Carpenter (2020) represents the most promising of such proposals, which is also nicely tailored for the conjunction assessment problem. While the theoretical development is indisputable, a couple of practical problems remain:

- First, the combination methodology relies directly on realistic covariances accompanying each state estimate. If these covariances are not representative, then the fused product is errant not just in its own covariance but in its synthesized state estimate. Because covariance realism is an elusive achievement for many providers, and because a rigorous V&V effort is required to establish the abiding presence of realistic covariances in a provider's product set, direct fusion is not a mechanism that can be easily or immediately employed.
- Additionally, the theory requires the cross-correlations between the covariance matrices arising from different providers to be characterized and deployed in the fusion paradigm, yet there is no obvious method for establishing these cross-correlations between the providers' orbital determination uncertainties. There is an argument that, due to the use of different input data with different errors, the correlated error should be negligible; at the same time, it could reasonably be expected that some shared model error, such as geopotential error or atmospheric density forecast error, would appear in a cross-correlation analysis.



So, for the direct fusion methodology described here, more focused study is needed before an approach of this type can be employed operationally.

Conclusion about the use of commercial SSA data

Given the present difficulties with the presence of multiple SSA and conjunction assessment products, NASA has concluded that it is necessary to limit the use of commercial SSA data to the combination of commercial and DOD tracking information.

L.2 Validate all non-SSN data

All non-SSN sources supplying data to be used in orbit determination solutions to maintain the catalog must be regularly calibrated to ensure the removal of any data biases that might skew the conjunction assessment screening results.

Using raw observation data from commercial vendors (as opposed to post-processed solutions) enables straightforward data characterization and numerical validation.

Commercial vendors supporting NASA are regularly asked to track and submit the tracking data taken on calibration satellites for which precision ephemerides are available; these satellites can be both dedicated calibration spheres (such as those used by the International Laser Ranging Service) and U.S. Government payloads with stable orbits. The commercial tracking data are compared to the precision ephemerides and the residuals characterized for each observable: mean errors can be subtracted from the data themselves and thus do not affect the data quality, error variances can be used as sensor data weighting factors in the orbit determination process, and non-Gaussianity and variation of the means and variances with time can indicate an unstable situation that may render a particular commercial provider's data unsuitable for use.

For stable commercial data sources, quantification of mean error and error variance allows the data to be combined with SSN data (which also have quantified error means and variances) to produce an orbit determination result that has weighted the constituent data correctly and thus properly considers the relative accuracy of the inputs in forming the desired single solution.

L.3 Undertake a cost/benefit analysis before purchasing commercial SSA data

While following the recommendations of L.1 and L.2 above would allow the introduction and proper use of commercial SSA data in NASA conjunction assessment, a third consideration focuses on whether the use of these data would in fact result in a significant operational benefit.

NASA, as a U.S. Government entity, follows the guidance of the National Space Policy to receive conjunction assessment services from the 18 SDS and 19 SDS, who maintain the U.S. catalog of space objects. While it is true that adding properly calibrated commercial tracking data should result in a more reliable orbit determination solution with a smaller uncertainty, the effect may be such that the use of these additional data would rarely, if ever, result in a different operational decision regarding whether to require and execute a conjunction mitigation action.



Most conjunction situations receive adequate SSN tracking data to the degree that adding some additional data does not change the risk assessment appreciably and therefore does not alter the operational decisions. A complex cost-benefit analysis would need to be performed to understand the financial obligation appropriate to purchase commercial data to augment the existing NASA conjunction assessment process based on the risk mitigation expected.

If, for example, having commercial data changed a conjunction P_c value from $5E-05$ to $1E-04$, this would cause a mitigation action to be taken when, without the data, it probably would not have been if the P_c threshold for maneuvering were set at $1E-04$, so the operational outcome was changed to lower the risk. However, the risk exposure if the mitigation action were not taken is still very low: an actual risk of a 1 in 10,000 chance of a collision versus the 1 in 20,000 chance calculated with the SSN data alone.

The benefit would depend on how many times per year these decisions would be altered and thus how much risk is mitigated. By some estimates, over 90% of the objects larger than 1cm and thus able to render a satellite inoperative in a collision are too small to be tracked and thus are not considered in the conjunction risk assessment process. Therefore, part of the trade space is to consider how much adding commercial data reduces collision risk compared to the background risk. This decision would likely vary by orbit altitude based on trackability of objects of various sizes and the existing debris population.



Appendix M. Use of the Probability of Collision (Pc) as the Risk Assessment Metric for Conjunction Assessment

M.1 Introduction

Satellite conjunction assessment comprises two principal goals: to protect important assets from premature and unplanned mission failure due to preventable collisions and to assist in the regulation and minimization of space debris production. The first of these goals is in its details largely left up to the individual O/O to adjudicate. After all, the particular “value” of any given on-orbit asset, and therefore the level of risk of its possible loss that one is willing to bear, are governed by the specifics of the situation including the age (and perhaps importance) of the satellite and mission, the degree to which the mission objectives have already been met, and mission redundancy provided by additional spacecraft. It is best left to the individual mission project office to choose appropriate conjunction assessment actions (or inactions) relating directly to mission preservation. However, the second goal of overall space debris production minimization is much broader in scope. Born of the desire to keep key orbital corridors free from debris pollution to allow their perpetual continued use by all space actors, this goal transcends the health and preservation of the individual mission. It is in response to this second goal that actual conjunction risk assessment and mitigation thresholds are articulated. Mission operators can always take a more conservative posture than what is appropriate for debris mitigation, but at the least they must embrace a minimum level of responsibility to preserve key orbital corridors for future use.

To this end, the purpose of satellite conjunction assessment and risk analysis is neither to maximize safety, nor fully to minimize risk of satellite conjunction with other objects, nor absolutely eliminate the likelihood of space debris production. Instead, the official CARA statement of purpose is more nuanced: to take prudent measures, at reasonable cost, to improve safety of flight, without placing an undue burden on mission performance. This statement includes a number of qualitative terms, such as “prudent,” “reasonable,” and “undue burden”; for ultimately, it is not a scientific conclusion but a series of prudential judgments to assemble guidelines that work to prevent space debris pollution while accommodating the competing claims of mission execution and inherent levels of risk assumed simply by launching a satellite at all.

It is this last consideration, namely the risk necessarily assumed simply by launching a satellite, that requires attention, especially in selecting a collision likelihood metric and evaluation paradigm. A 2020 NASA ODPO space debris catalog generated for CARA contained over 300,000 objects larger than 1 cm in physical size, which is the level at which an object is typically considered able to penetrate a satellite’s shielding and render it inoperative. With tracking improvements and the launch of additional satellites, one can expect a regularly maintained space catalog of perhaps 30,000 to 50,000 objects. This means that, roughly speaking, about five-sixths of the objects large enough to leave a satellite in a failed and uncontrolled state if a collision should occur with them will be untracked. Presumably, that same proportion of the close-approach events that actually occur are not discoverable with current sensor technology and cannot be mitigated. Given then that only about one-sixth of the close-



approach events are trackable and in principle actionable, the overall conjunction risk analysis process (and the risk assessment parameters that drive it) should be commensurate with a situation in which greater than 85% of similarly likely collisions cannot be addressed at all and thus constitute a risk that simply has to be accepted. It is not reasonable to adopt an excessively conservative risk management position for known conjunctions when so substantial a portion of the actual collision risk is accepted without any possible mitigation as part of the cost of space operations.

However, despite the large background collision likelihood that is accepted simply by launching a satellite at all, there is still great value to on-orbit conjunction analysis, risk assessment, and mitigation. First, because collisions between protected payloads and large secondary objects will produce, by several orders of magnitude, the most debris fragments, there is substantial benefit to avoiding collisions of this type. These large secondary objects are resident and well maintained in the present satellite catalog, so they represent rather straightforward cases for conjunction assessment. Second, when serious conjunctions of any type are identified and are well understood, these also represent straightforward situations for which due diligence counsels risk assessment and possible mitigation action. It is only when the situation is poorly determined—when some information about a conjunction is present but not of the sufficiency needed to conclude that a problematic situation is in fact at hand—that requiring remediation actions through an overweening conservatism is not appropriate, given the size of the accepted background risk.

The purpose of this appendix is to explain the selected risk assessment metric and interpretive framework for that metric, chosen to enable proper balance between mitigation of truly problematic conjunctions and an unnecessary conservatism that reduces spacecraft lifetime and unduly encumbers science mission objectives.

M.2 Point of Reference: Conjunction Risk Assessment Based on Miss Distance

In the early days of conjunction assessment, satellite position uncertainty data were not regularly available, so the only orbital data product on which to base conjunction risk mitigation decisions was the predicted miss distance at TCA between the two conjuncting satellites. If the miss distances were smaller than the combined sizes of the two objects (a quantity usually on the order of 10-20 meters), then it was clear that a mitigation action would be necessary to modify the primary satellite's orbit to increase this miss distance to a safe level. But it was also known that there was often significant uncertainty in the two objects' predicted state estimates, so miss distances that were larger than the objects' combined size were also likely to be threatening—but how threatening, precisely? Similarly, if a mitigation action such as a maneuver were pursued, how large should such an action be to guarantee a desirable level of safety? Because the answers to these questions were not known, very conservative miss-distance thresholds were then embraced, often based on very little analysis, which led to a great deal of operational anxiety and unnecessary mitigation actions. For example, nearly all conjunctions with miss distances (at TCA) less than a value of 5 km present perfectly safe encounters, but all of these could be treated as worrisome and worthy of potential mitigation actions. Such a situation could not be sustained operationally: it went beyond prudence and presented an undue burden to mission operations.



Methods were thus developed that considered the characterized error in the state estimates to determine the likelihood that the two trajectories at TCA would have a close approach smaller than the combined sizes of the two satellites.

Approaches that view the problem in this way, namely those that give an actual likelihood that the miss distance will be small enough to cause a collision, are certainly an advance over the use of the miss distance alone. It is important to remember, however, that the probabilistic answer they produce is solely a function of the quality of the astrodynamics data that are used as input to the computation—the tracking information available and the errors encountered in predicting states from epoch to TCA. In truth, the probability of collision for any given conjunction is actually either 1 or 0: the conjunction is either going to result in a collision, or it is not. The probabilistic framing comes from the degree of predictive certainty of the outcome brought by the quality of the astrodynamics data in the particular case. There is no “definitive” collision likelihood value for a particular conjunction. Improvements in data and data quality will push the calculated answer further toward the values of 0 or 1 depending on whether the two satellites actually are on path to collide, and because satellite collisions are extremely rare events, in nearly every case the true likelihood of collision is 0. Sometimes interest is expressed in wishing to obtain sufficient tracking data to allow the “true” collision likelihood to be calculated, or after the event, to rework the solution using the tracking data collected *ex post facto* to establish what the “definitive” collision likelihood actually was. None of these considerations is in the end helpful, or for that matter even possible. In the first case, while more and better data will provide a superior answer, any value short of 0 or 1 is just an estimate constrained ultimately by the inadequacy of the tracking data. In the second case, the *ex post facto* solution is not definitive but is yet another estimate, this time with somewhat better input data. The probabilistic framework is helpful and desirable, but in the end, it reflects what is known about the conjunction situation rather than being a stand-alone, absolute assessment of collision likelihood.

M.3 Use of Pc for Conjunction Risk Assessment Requirements

Many conjunction risk assessment metrics that have been proposed in the critical literature; Hejduk and Snow (2019) give a useful overview, description, and attempted categorization. In choosing a particular collision likelihood metric for requirements specification purposes, different considerations, technical and otherwise, are relevant:

- Suitability to NASA’s risk posture regarding conjunction risk assessment;
- Ability to represent the collision likelihood in a manner commensurate with this risk posture;
- Straightforwardness and tractability of calculation;
- Ease of conceptual grasp of the metric and its origins; and
- Acceptance within the conjunction assessment industry.

From these considerations, CARA has chosen the Probability of Collision (Pc) as the metric for high-risk conjunction identification. Of the different options examined, this metric was the best candidate to evaluate collision risk given the desired context of balancing safety of flight with minimizing the disruption of mission objectives. It is straightforward to calculate and, with certain recent improvements, can be computed quite accurately in many astrodynamically



demanding circumstances. It can be explained relatively easily to, and be interpreted by, decision makers. It can be turned into a statement about miss distances if this framework is desired. Finally, it is the emerging metric of choice among the military, civil, and commercial conjunction assessment industries.

The P_c metric, as calculated by analytic methods, was first explained formally in 1992 (Foster and Estes). A comprehensive treatment of the calculation and associated issues can be found in Chan (2008), although this monograph is now somewhat dated and does not consider many of the newer collision likelihood calculation proposals. (See Appendix K for an explanation of the presently embraced calculation methods for this parameter, along with the tests that have to be performed to determine which calculation approach to use in any particular case. It may be helpful to the reader new to conjunction assessment to refer to Appendix K before proceeding as it gives a precise definition of terms used in the following treatment.)

M.4 P_c and Probability Dilution

Despite the previous section's account of selecting a metric, the P_c is not a parameter without controversy. The main objection to the metric is a phenomenon called "probability dilution" in which low values of the P_c do not necessarily guarantee safety although they can offer support for refraining from a mitigation action. This section discusses the overall phenomenon of probability dilution and explains why it is viewed as a manageable issue when using the P_c in mitigation threshold development.

As stated previously, probabilistic conjunction assessment metrics take on their probabilistic nature from the uncertainties in the state estimation data used to characterize the miss distance at TCA. It is not difficult to understand the alignment of inputs that creates a high P_c value: the calculated miss distance between the two objects is small, and the primary and secondary object covariances (and thus the uncertainty on the miss distance) are reasonably small also, so one easily envisions that of the entire set of possible actual miss distances, some notable portion will be smaller than the hard-body radius. The P_c , which is the portion of the possible miss distances smaller than the hard-body radius, will be relatively large. Imagine a similar situation for a small P_c : the nominal miss distance is large, and the covariances and miss-distance uncertainty are small, so the range of possible actual miss distances are nearly all rather large. One can conclude quite satisfactorily in such a case that there is little chance that the actual miss distance will be less than the hard-body radius.

But what if, for either of the previous cases, one or both covariances are extremely large? This would happen if, for at least one of the satellites, the predicted position at TCA, due either to a poor orbit determination update or difficulties in accurate propagation, were extremely badly known. The predicted miss distance is by definition the expected value, but it is a poor proximate prediction of the miss distance because there is so much uncertainty in one or both of the satellites' position at TCA. The range of possible miss distances now becomes extremely large. Therefore, a relatively smaller portion of the possible miss-distance values will be smaller than the hard-body radius, and the P_c will take on a small value. In the earlier case in which the nominal miss distance was large but the covariances small, one could with confidence conclude, based on the quality of the data, that a collision is unlikely. In this latter case, the likelihood of



collision is also small, but only because one has very little idea where one or both satellites actually will be at TCA, so one cannot conclude that a small miss distance is likely when so large a range of miss distances is possible. This latter case is called “probability dilution” (a term introduced by the first treatment of this subject in the literature (Alfano 2005b)) because the small value of the P_c is not achieved by the certainty of well-established state estimates but through “dilution” by relatively poor state estimates.

An analogy that is sometimes helpful is that of determining whether two cars parked in a large parking lot are parked next to each other. If one knew that one car was parked on the left side of the parking lot and the other on the right side of the parking lot, then one could conclude that it is unlikely that the two cars are parked next to each other: only if both cars park on the boundary between the left and right sides, and then only if they actually choose adjacent spaces, will the two cars be parked next to each other. This is a conclusion enabled by the definiteness of the data. Now, suppose that one knows nothing at all about where the two cars are parked in the parking lot; what is the likelihood of their being parked next to each other? It is also low, but in this case not because one knows that the cars have been placed in different parts of the lot but rather because, in a large parking lot, it is simply unlikely that any two cars will happen to be next to each other. It is a conclusion that follows not from what is known but rather from what is not known; one cannot conclude from the available data that the cars are probably far apart; but at the same time there is no evidence to indicate that they are close. If, therefore, one is required to hazard a guess, the large size of the parking lot makes the supposition that they are not adjacent reasonable.

So, what is the risk assessor to do in such a situation? One could embrace a very conservative position and require that, unless it can be demonstrated conclusively that the two satellites are virtually certain not to collide, a mitigation action is warranted. Some commentators have suggested this position as the natural one for advancing safety of flight (e.g., Balch et al. 2019). There are two sets of difficulties with such a position, one of which is practical and the other conceptual.

The practical difficulty centers on the number of increased mitigation actions and the magnitude of those actions if an extremely conservative risk analysis metric/approach were to be embraced operationally. An analysis by Hejduk et al. (2019) indicated that, for a protected asset in a 700 km circular orbit, the adoption of the conservative “ellipse overlap” technique, for which the two covariances’ overlap has to be limited to a very small value to certify that a collision is extremely unlikely, would increase the number of mitigation actions by a factor of anywhere from 6 to 10. Most O/Os believe they are already assuming a relatively safe posture in that they have set the thresholds on the risk-assessment metrics they currently use to require mitigation actions close to the mitigation action rate that they believe they can sustain without unacceptable mission disruption. While perhaps a relatively bounded increase could be countenanced, any expansion beyond that would be extremely difficult to accept. Increases by a factor of as much as an order of magnitude simply cannot be borne without resulting in major disruption, if not nullification, of the mission activities that most satellites are launched to perform. Furthermore, remediation actions based on minimizing covariance ellipsoid overlap rather than reducing the P_c value to an acceptable level will need to be large—much larger than the typical satellite maneuvers that are



presently performed. Large maneuvers expend additional fuel and, if pursued more frequently, will also require subsequent response maneuvers to restore the orbital parameters that were violated by the initial mitigation action. An extremely conservative risk analysis approach such as the one described here is simply not seen as operationally viable for most missions.

In addition to these practical impediments, a conceptual dissonance is introduced in embracing an extremely conservative risk-assessment strategy given the much larger collision background risk from untracked/uncataloged objects. As previously explained, the dynamics of the dilution region result in a reduction in severity and therefore a reduction in perceived necessity to act as less is known about the conjunction. As the amount of tracking information (or, similarly, the amount of certainty in prediction) for a dilution-region conjunction is worsened, the satellite covariance(s) increase in size, and the P_c decreases until ultimately it results in a value of 0 (to machine precision). This asymptotic value of nullity aligns nicely with the zero-value P_c that is, at least indirectly, imputed to conjunctions with untracked/uncataloged objects and about which the risk-assessment analyst can do nothing at all. As one progresses from knowing a lot, to a little, to nothing at all about a conjunction, the P_c moves conceptually from a higher value, to a lower value, to a zero value. For an extremely conservative approach such as that of minimizing covariance ellipsoid overlap, an opposing and inconsistent dynamic is observed: the less one knows about the conjunction, the larger the covariance ellipsoids are, and therefore larger and more frequent maneuvers are required to achieve minimum ellipsoid overlap to ensure safety until one moves from knowing a small amount about a conjunction to knowing nothing at all, and then—there is a sudden disjunction from taking large and invasive actions to doing nothing. Given that, as stated previously, about 85% of the conjunctions that a satellite actually faces cannot be addressed at all because nothing is known about them, it does not make sense that, for the small number of conjunctions for which only poor data are available, large and disruptive mitigations are required.

Instead, the use of the P_c , with the dilution region dynamic explicitly recognized, is a more natural fit for the situation that is actually encountered. When outside the dilution region, a satisfactory amount of orbital data and reasonably small covariances exist. In this situation, the P_c accurately reflects a situation that is either worrisome or safe, and one can be confident in the conclusion in either case. If in the dilution region the P_c is high despite the poor data quality and large covariances, a worrisome situation has very much been identified, so appropriate mitigation action should be taken. If in the dilution region the P_c is low, one cannot, as has been explained previously, necessarily infer that the situation is safe; the two satellites might actually be poised for a dangerous close approach with this fact obscured by poor data quality—a situation that could potentially be revealed by the summoning of additional tracking data. It is appropriate to recognize that this situation (state estimate with large covariance) is not dissimilar to that of a conjunction with an untracked/uncataloged object about which nothing is known (random state estimate and infinite covariance). It is thus acceptable to treat low- P_c dilution region cases as a small extension of the untracked/uncataloged object conjunctions and not pursue a mitigation action. Requiring conjunction remediation for low- P_c cases with poor data quality when such cases are truly very similar to the ~85% of conjunctions that are believed to exist but for which no mitigation is possible is not considered to be a prudent measure and thus runs counter to the CARA statement of purpose.



While not appropriate for broad implementation, conservative approaches such as ellipsoid overlap minimization are not without merit. In situations in which the collision risk may be pushed higher by other factors, such as a high-consequence conjunction due to the potential to produce large amounts of debris, it may be desirable to employ a conservative method when in the dilution region. In such a case, one might first analyze the situation by manipulating the covariance and determining the highest P_c value that could be realized with the miss distance (following Alfano 2005b); if that P_c is still below the threshold, then the conservative approach would be difficult to justify. But if this “maximum P_c ” is above the threshold, then the conjunction could in fact be worrisome, and a conservative approach could be properly applied. At a minimum, if it were possible to marshal additional tracking data to improve the state estimate, then a situation such as this would be a good fit for employing such a capability.

Finally, it should be noted that there have been interesting proposals recently for risk assessment approaches based not on the probability of collision but on the (somewhat) related concept of examining confidence intervals on the miss distance; such proposals include those of Carpenter (2019) and Elkantassi and Davison (2022). These approaches, which are presently being evaluated formally, bring the advantage of avoiding situations in which, with relatively small miss distances, even risky conjunctions might be obscured by the inability, due to largish covariances, to integrate up enough risk to register as problematic events that require mitigation. However, the expectation is that using such approaches will produce unacceptably large false alarm rates, and the issue of “missing” high-risk events in low-miss-distance situations can be addressed by adding a miss distance mitigation criterion in addition to that based on the P_c . But any firm recommendations will need to wait for the completion of a full analysis.

M.5 Conclusion

It is emphasized that the above guidance describes and explains why P_c was chosen by NASA CARA as the risk-assessment metric to be used to determine the circumstances under which a mitigation action is required of missions to promote preservation of orbital corridors from debris pollution. O/Os may always pursue additional mitigation actions in a manner that increases the conservatism of their safety profile. For the case of low- P_c conjunctions in the dilution region, missions may elect to pursue mitigation actions. They may even use extremely conservative methods such as ellipsoid overlap minimization to size these mitigation actions. This guidance indicates that mitigation actions are required only when the P_c exceeds the appropriate mitigation threshold. Missions may always pursue additional such actions, either episodically or as part of a standing strategy, if they wish a more risk-adverse safety posture.



Appendix N. Pc Calculation Approaches

N.1 Introduction

This appendix discusses the selection of the Probability of Collision (Pc) as the risk assessment parameter to use for conjunction assessment requirements compliance. While this parameter is widely used in the conjunction assessment industry, issues related to its calculation exist that merit extended discussion. The most frequently used analytical techniques to calculate the Pc are well established and computationally efficient but include assumptions that restrict their use and make the calculations vulnerable to error for a small fraction of conjunctions. Numerical techniques also exist, such as Monte Carlo Pc estimation. Predictably, these make fewer assumptions and are more widely applicable, but they are much more computationally demanding. There are also issues related to the regularization and interpretation of the input data to the Pc calculation, some of which are resolved by techniques that are now becoming standard practices. In calculating Pc estimates, it is necessary to examine and prepare the input datasets carefully and then to choose the calculation approach that is appropriate to the situation. The purpose of this appendix is to amplify the Pc calculation-related recommendations by providing an extended technical explanation of the data preparation and Pc calculation issues so that implementers and users of these calculations can proceed with a better understanding of the different options and resultant fidelities of Pc calculation.

To accomplish this goal, this appendix will address the following technical areas:

- A step-by-step description of the conjunction plane two-dimensional Pc calculation, which is the most established and widely used analytical Pc computation technique, and its enabling simplifications and assumptions;
- Examination and repair/expansion of input data to the calculation, focusing mostly on the orbital state covariance matrices for the two objects in conjunction;
- Discussion of the use of Monte Carlo techniques, which is the numerical method used for high-fidelity Pc computation;
- A test to determine whether an analytical or numerical technique should be used for a particular conjunction;
- Approaches to choosing for the Pc calculation the hard-body radius, which gives a statement of the combined sizes of the primary and secondary objects; and
- Discussion of alternative analytic Pc calculation methods, specifically the two- and three-dimensional “Nc” (as opposed to “Pc”) estimation methods that address conjunctions affected by curvilinear trajectories and non-Gaussian distribution effects.

N.2 Conjunction Plane Analytic Pc Calculation

The conjunction plane method of Pc calculation, which is by far the most widely used approach in the conjunction assessment industry, was developed for the Space Shuttle Program and first described in the literature in 1992 (Foster and Estes). There have been a number of important



treatments since that time — e.g., Akella and Alfriend (2000), Patera (2001), Alfano (2005a), Chan (2008), Garcia-Pelayo (2016), and Elrod (2019) — but all rely on the same basic methodology: applying reasonable assumptions to enable analytical approximations. While the particulars vary, these approaches all share the same concept of calculating the P_c estimate by integrating over a two-dimensional region on a conjunction encounter plane.

Conjunction plane P_c analysis begins with the states and covariances for the primary and secondary objects' orbital states at TCA. An important set of questions should be addressed concerning whether these data, especially the covariances, are truly representative of the expected states and uncertainties at TCA or whether the propagation process has distorted them. These questions will be addressed in a subsequent section, once a more focused context for them has been established through the present discussion of the general procedure.

The first step is to recognize that P_c calculations depend on the relative positions and uncertainties of the two objects, so moving to a framework that views the problem this way is helpful. Subtraction of the two objects' positions produces a relative position vector, the magnitude of which is the miss distance between the two objects (at TCA). Similarly, because interest is in the relative rather than absolute position uncertainty, it is possible to combine the two objects' covariances to form a joint (relative) covariance and allocate that, if desired, to one "end" of the relative position vector (by convention the end for the secondary object), as shown in Figure N-1. There are, of course, questions regarding whether the two covariances are independent and can be combined by simple addition; this question is addressed in a later section, but it is typically acceptable to presume independence and combine the covariances in this manner.

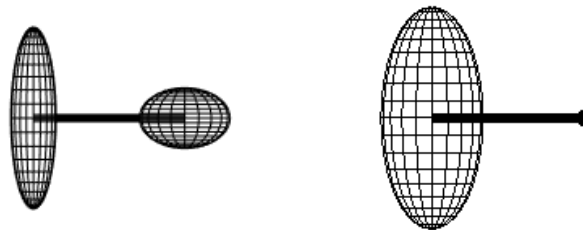


Figure N-1 Relative Positions and Uncertainties of Two Objects

The second step relates to modeling the combined sizes of the primary and secondary objects. The general approach is to place a circumscribing sphere about the primary (whose size is well known by the O/O because it is their satellite) and then do the same thing for the secondary but often via an estimation technique as the secondary is usually a debris object for which there is no definitive size information. If these two spheres approach and begin to overlap one another at any point during the encounter, then a potential collision has been identified. Again, keeping in mind that a relative framework is useful here, the two objects' size spheres can be combined into one super-sphere (also called the "collision sphere") and placed at one end, by convention the primary object end, of the relative miss vector, as shown in Figure N-2. If the miss vector should shrink to be smaller than the radius of the collision sphere (also called the hard-body radius), that would be the equivalent of the two original spheres encroaching on each other at TCA.

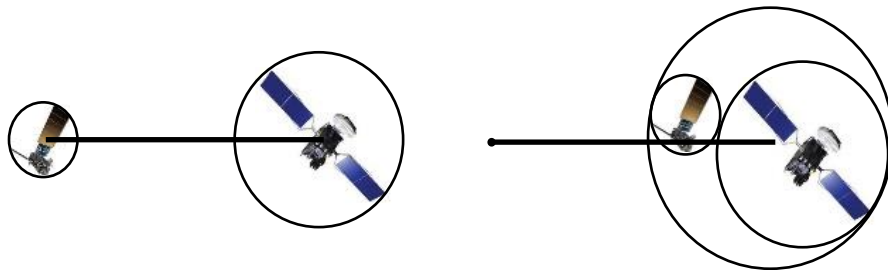


Figure N-2 Combining the Sizes of the Primary and Secondary Objects

The third step is to envision the situation at TCA in which all the uncertainty is assigned to the secondary object's end of the relative miss vector held in a fixed position in the mind. The primary object end of the relative miss vector is moving along through TCA and bringing with it the sphere representing both objects' combined size. Even though the satellites follow curved trajectories and the covariance evolves and changes at each instant, if the encounter is presumed to take place extremely quickly—and this is in most conjunctions a good assumption because the satellites' relative velocity usually exceeds 10 km/sec—then two assumptions can be made: the trajectories are essentially rectilinear during the encounter period, and the covariances (and thus the joint covariance) can be considered static. This means that the encounter can be envisioned as in Figure N-3:

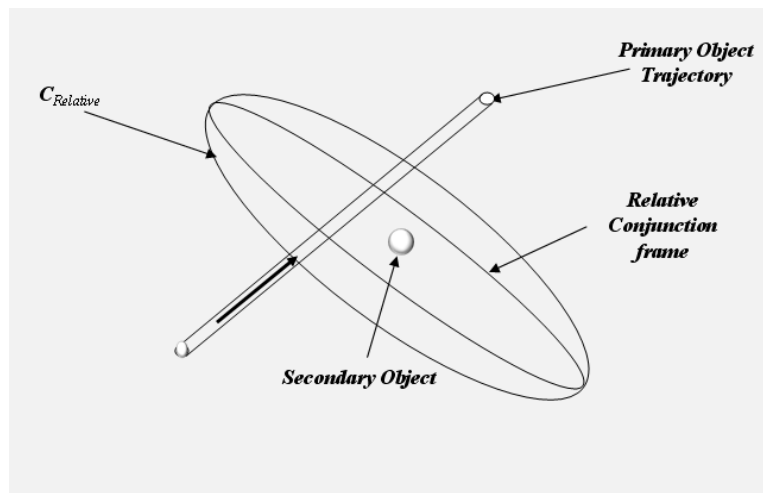


Figure N-3 Geometry at TCA

The passing of the primary object by the secondary can be seen as following a “soda straw” straight trajectory whose cylindrical radius is the same as that for the hard-body radius and whose placement is one miss distance away from the position of the secondary at TCA. Since the joint covariance shown as the ellipsoid above represents the uncertainty of one “end” of the miss-distance vector (as shown by the central dot in the above diagram), this dot can be presumed to be potentially in any place within the ellipsoid, meaning that in some portion of those realizations, it will fall within the soda straw. When this is the case, a collision is presumed. The task is to determine the likelihood that the dot will, in the actual realization of this



conjunction, fall within the cylindrical path (“soda straw”) swept out by the motion of the primary object. This probability can be decomposed to be rendered as the product of the individual probabilities that each component of the secondary object position (the dot) will fall within the soda straw pathway, i.e., if an orthogonal x-y-z coordinate system is presumed, this overall probability can be generated as the product of the probability that the x-component of the dot’s position will fall within the straw, the y-component of the dot’s position will fall within the straw, and the z-component of the dot’s position will fall within the straw. If this coordinate system is aligned so that one of the axes (e.g., the z axis) aligns with the direction of the straw, because one is assuming rectilinear motion, the soda straw can be presumed to be unbending and infinite in length, and as such, it will contain all of the z-component probability of the dot’s falling within the straw. As such, the z-component probability in this arrangement will be unity and will be what is called “marginalized out,” meaning that the overall probability can be fully represented by the probability remaining with the x- and y-components. The entire situation can thus be reduced from three to two dimensions and analyzed as a phenomenon that occurs on a plane that is orthogonal to the soda-straw direction, which is the direction of the relative velocity vector. This procedure defines the “conjunction plane,” which can be viewed in two equivalent representations as discussed by Chan (2008, see Figure 5.1), and as shown in Figure N-4.

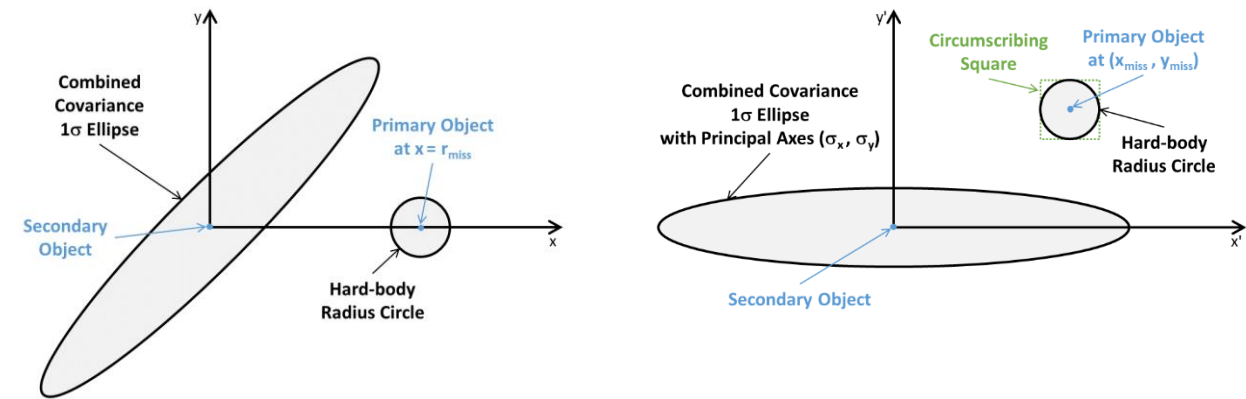


Figure N-4 Two Equivalent Representations of the Conjunction Plane

In the first representation, shown in the left panel of Figure N-4, the center of the secondary object is placed at the origin, and the local (x, y) coordinate system configured so that the miss vector (which extends a distance of r_{miss} from the secondary to the primary object) lies along the horizontal x axis. The “soda straw” is coming out of the page and represented as the hard-body-radius circle. With this planar reduction, the P_c is now the frequency with which the miss-distance vector will fall within the hard-body-radius circle; this is equivalent to the amount of joint covariance probability density (illustrated here using a 1σ ellipse) falling within that circle. Since the projected joint covariance represents a bivariate Gaussian distribution, the amount of its probability density falling within the hard-body-radius circle is given by the following two-dimensional integral (Foster and Estes, 1992)

$$P_c = \frac{1}{\sqrt{\det(2\pi C)}} \iint_A \exp\left(-\frac{\mathbf{r}^T \mathbf{C}^{-1} \mathbf{r}}{2}\right) dx dy \quad (\text{N-1})$$



in which \mathbf{r} is the 2×1 miss vector, C is the 2×2 covariance matrix, and A is the hard-body-radius circular area. There are several different approaches to evaluating this integral. Foster and Estes (1992) applied a two-dimensional quadrature technique; this works well, and MATLAB®’s¹³ adaptive *quad2d* integrator is quite equal to the task, although perhaps not the most computationally efficient of all possible choices. Chan (2008) uses equivalent-area transforms to produce a single-dimensional integral, which has a series solution. Garcia-Pelayo et al. (2016) also derives a multi-term series approximation. However, even though these series approximations are relatively computationally efficient, experience indicates that they occasionally produce inaccuracies. Elrod (2019) formulates the integral in terms of complementary error functions (to improve accuracy for conjunctions with small P_c values) and uses Gauss-Chebyshev quadrature with nodal symmetry (which improves the efficiency of the numerical integration considerably). The Foster and Elrod approaches (the former being the established standard, and the latter being extremely fast, especially with a vectorized MATLAB implementation) are included as the *Pc2D_Foster* and *PcElrod* functions in the *Pc Computation Software Development Kit (SDK)* in the NASA CARA software repository. (See Section 7, Contact Information in this document for the specific URL.)

In the second conjunction plane representation, shown in the right panel of Figure N-4, the secondary object location again is placed at the origin, but in this case the local (x', y') coordinate system is configured so that the principal axis of the covariance ellipse lies along the horizontal axis. The center of the primary object lies at (x_{miss}, y_{miss}) , and the axes are oriented so that this miss position lies within the 1st quadrant, so that $x_{miss} \geq 0$ and $y_{miss} \geq 0$. Using this representation, the P_c is given by a one-dimensional integral involving error functions (Alfano, 2005a)

$$P_c = \frac{1}{\sqrt{8\pi}\sigma_x} \int_{-R}^R \{\text{erf}(y_+) - \text{erf}(y_-)\} \exp\left[-\frac{(u + x_{miss})^2}{2\sigma_x^2}\right] du \quad (\text{N-2})$$

with R indicating the combined hard-body radius, $u = x' - x_{miss}$ the integration variable, and $y_{\pm} = (y_{miss} \pm \sqrt{R^2 - u^2})/(\sqrt{2}\sigma_y)$. The integrand factor in the curly brackets represents the difference of two error functions, $\Delta = -\text{erf}(y_-)$. In many software environments (e.g., MATLAB), this factor often can be computed significantly more accurately as a difference of complementary error functions, i.e., $\Delta = \text{erfc}(y_-) - \text{erfc}(y_+)$, especially when calculating very small P_c values (Elrod, 2019). See Abramowitz and Stegun (1970) and Press et al. (1992) for details on computing $\text{erf}(-)$ and $\text{erfc}(-)$ functions.

For most conjunctions, Gauss-Chebyshev quadrature provides an efficient and accurate means to calculate the one-dimensional integral in equation (N-2), using an approach similar to that described by Elrod (2019). However, for conjunctions involving relatively large hard-body radii (or, equivalently, small covariance ellipse σ_x dimensions), this method can potentially become inaccurate. Specifically, Gauss-Chebyshev quadrature becomes increasingly inaccurate as the hard-body radius grows beyond the limit $R_{lim} = 4\sigma_x - \min(R)$. In such cases, which rarely occur in practice, an adaptive numerical integrator can be used to calculate an accurate estimate, e.g., MATLAB’s *integral* function. (The function *PcConjPlaneCircle* of the NASA CARA SDK

¹³ MATLAB is a registered trademark of The MathWorks, Inc.



repository implements a vectorized algorithm that automatically determines which of these two integration methods should be used to compute P_c values accurately for all input hard-body radii and covariance values, with a computation speed comparable to that of the *PcElrod* function for most conjunctions. Also, for cases that have hard-body radii well below the limit given above, testing indicates that the SDK functions *Pc_Foster*, *PcElrod*, and *PcConjPlaneCircle* all output nearly identical numerical P_c values, i.e., that typically agree to five digits of precision or more.)

The second conjunction plane representation shown in the right panel of Figure N-4 also provides an extremely efficient means to calculate an upper limit estimate for the P_c value. This upper bound corresponds to the two-dimensional (2-D) integral over the square that circumscribes the hard-body radius circle (as shown in Figure N-4), which has the following analytical solution

$$P_c < P_{sq} = \frac{[\text{erf}(X_+) - \text{erf}(X_-)][\text{erf}(Y_+) - \text{erf}(Y_-)]}{4} \quad (\text{N-3})$$

with

$$X_{\pm} = \frac{x_{miss} \pm R}{\sqrt{2}\sigma_x} \quad \text{and} \quad Y_{\pm} = \frac{y_{miss} \pm R}{\sqrt{2}\sigma_y} \quad (\text{N-4})$$

Again, in many cases the $\text{erf}(-)$ differences in equation (N-3) can be computed more accurately using $\text{erfc}(-)$ differences. Notably, the circumscribing square probability estimate does not require any numerical integration at all, but instead only requires the computation of four $\text{erf}(-)$ or $\text{erfc}(-)$ functions, usually making it relatively easy to program into software and significantly more computationally efficient. These considerations could be important in some circumstances (e.g., for computations performed on orbiting satellites), prompting the use of P_{sq} as an approximation for P_c itself. For instance, CDMs generated by the USSPACECOM ASW processing system often reports P_{sq} as the estimate of conjunction's collision probability. (An optional, non-default mode of the function *PcConjPlaneCircle* in the NASA CARA SDK repository implements an efficient vectorized algorithm that calculates P_{sq} values).

It is perhaps helpful at this point to review the four assumptions employed by the conjunction plane P_c calculation methods given by equations (N-1) through (N-4), because alternative P_c estimation techniques will be needed when these assumptions do not inhere:

1. Statistical Independence: The two objects' uncertainty distributions are statistically independent so that the joint covariance can be obtained by simple addition of the two covariances. This assumption is largely true but can break down for objects that share global atmospheric density forecast error in a manner that influences the conjunction. This issue will be discussed as an isolated topic in a subsequent section of this appendix.
2. Rectilinear Motion: The conjunction circumstances are such that it is reasonable to presume rectilinear motion and static covariances during the encounter. These conditions inhere for most conjunctions between Earth-orbiting satellites. The objects' relative velocity at TCA is in some places used as an indication of the reasonability of these assumptions, but this



parameter alone is not sufficient to identify situations in which the conjunction plane P_c approximation will miscarry.

3. Gaussian Position Distributions and Negligible Velocity Uncertainties: The position vector state errors for each satellite at TCA follow Gaussian distributions, and the velocity vector state errors are negligibly small. When combined, these assumptions lead to the conjunction plane representations shown in Figure N-4. Conjunctions that do not satisfy these assumptions are addressed by alternate analytical and Monte Carlo methods, discussed in the sections below.
4. Temporally Isolated Event: The conjunction presents a single, well-defined event so that the collision likelihood can be ascertained by examining that single instance. Objects that stay in close proximity for extended periods accumulate risk throughout long interactions, rather than quickly accumulating risk at or near a well-defined TCA. A different approach is also required for their evaluation, which is discussed in the sections below.

As mentioned previously, the issue of statistical independence (i.e., assumption 1 above) will be discussed in a subsequent section of this appendix. To address conjunctions that do not satisfy any of the other assumptions, two alternative (but more computationally intensive) analytical methods are available: the “three-dimensional N_c ” method, which research indicates can be applied to conjunctions that violate assumptions 2, 3 and/or 4 above, and the “two-dimensional N_c ” method, applicable to temporally isolated conjunctions that violate assumptions 2 and/or 3. Notably, the three-dimensional N_c method could, in principal, be applied to all conjunctions to estimate P_c values. However, this is not justified because most LEO satellite conjunction P_c values can be estimated accurately using the much more efficient conjunction plane methods described above. Additionally, most of the remaining conjunctions can be estimated accurately using the two-dimensional N_c method, which, although much slower than the conjunction plane methods, is still significantly faster than the full three-dimensional N_c method. (The function *PcConjPlaneUsageViolation* soon to be posted on the NASA CARA Software Development Kit (SDK) repository provides an algorithm that determines if a given conjunction violates one or more of conjunction plane P_c estimation assumptions, and if so, which of the other available P_c estimation methods are appropriate.)

N.3 Three-Dimensional N_c Method Analytic P_c Calculations

The relatively infrequent conjunctions that do not satisfy the conjunction plane method assumptions discussed in the previous section must be addressed with a different methodology, and in response to this need, several authors have formulated semi-analytical approaches relaxing some or all of these assumptions. Coppola (2012) proposed a method for single encounters designed to account for non-linear orbital motion and velocity uncertainties, resulting in an approximation for the probability rate, $\dot{P}_c(t)$, calculated using integration over the surface of a unit sphere. When combined with a one-dimensional time integration, this yields a “three-dimensional P_c ” approximation. Chan (2015) contested Coppola’s formulation, arguing that a proper approach must employ a set of random variables associated with a time-invariant Probability Density Function (PDF). NASA CARA implemented the three-dimensional P_c method in software (Hall et al. 2017a) and subsequently discovered that, for some conjunctions,



it can produce P_c estimates that differ significantly from high-fidelity Monte Carlo P_c calculations, even though all the required three-dimensional P_c assumptions are satisfied.

Shelton and Junkins (2019) provided a key insight into why the original three-dimensional P_c approximation fails in certain situations. Their analysis indicates that accurate P_c approximations require that the state uncertainty PDFs of the two satellites be estimated accurately *in the volume of space where they overlap the most*. The original Coppola (2012) three-dimensional P_c formulation did not incorporate this concept, but Hall (2021) reformulated the method to do so explicitly. For single encounters, the reformulated approach approximates the curvilinear motion of each satellite using a first-order Taylor series expansion, not centered on the mean orbital state, but centered instead on a state that coincides with the maximum overlap of the PDFs for the two satellites. The analysis demonstrates that such “peak overlap” states can be determined using an iterative calculation that converges quickly. The formulation derives an expression for “ N_c ”—the statistically expected number of collisions—which equals P_c for single, temporally isolated conjunctions, but that may exceed P_c for multi-encounter interactions. The resulting “three-dimensional N_c ” method entails a total of three numerical integrations, one over time and two over the surface of a sphere. The outermost, time integration expression has the form

$$N_c(\tau_a, \tau_b) = \int_{\tau_a}^{\tau_b} \dot{N}_c(t) dt \quad (\text{N-5})$$

This expression estimates $N_c(\tau_a, \tau_b)$, the number of collisions statistically expected to occur at some time during the risk assessment interval $\tau_a \leq t < \tau_b$, which can represent either a short duration closely bracketing a single close-approach encounter, or an extended duration spanning multiple encounters. The expected collision number is closely related to the collision probability. In fact, they are equal for single, isolated encounters between well-tracked satellites. The collision rate for such a temporally isolated conjunction is expressed as a two-dimensional integral over the unit sphere

$$\dot{N}_c(t) = R^2 \int_0^{2\pi} \int_0^\pi [v_t(\hat{\mathbf{r}}) MVN(R\hat{\mathbf{r}}, \check{\mathbf{r}}_t, \tilde{\mathbf{A}}_t)] \sin(\theta) d\theta d\varphi \quad (\text{N-6})$$

In this equation, the radial unit vector is given by $\hat{\mathbf{r}} = [\cos(\varphi) \sin(\theta), \sin(\varphi) \sin(\theta), \cos(\theta)]^T$, so the surface of the unit sphere is spanned by the azimuthal angle $0 \leq \varphi < 2\pi$ and the axial angle $0 \leq \theta \leq \pi$. The leading factor of R^2 represents the square of the combined hard-body radius, meaning that the expression actually represents an integration over the surface area of the collision sphere. As explained in Hall (2021), the integrand function in the square brackets is the product of two factors. The first is an average velocity term, $v_t(\hat{\mathbf{r}})$, which is a function of time (as indicated by the t subscript) and calculated using the TCA states and covariances of the primary and secondary objects. The second factor, $MVN(R\hat{\mathbf{r}}, \check{\mathbf{r}}_t, \tilde{\mathbf{A}}_t)$, represents a multi-variate normal (MVN) function which depends on $\hat{\mathbf{r}}$ and R , as well as a 3×1 relative position/velocity state vector, $\check{\mathbf{r}}_t$, and an associated 3×3 $\tilde{\mathbf{A}}_t$ covariance matrix, both of which are also calculated from the TCA states and covariances. Lebedev quadrature (Lebedev and Laikov, 1999) provides an efficient method for numerical integration over the unit sphere. (The function *Pc3D_Hall* of



the NASA CARA SDK repository computes conjunction P_c estimates, along with associated N_c and N_c rate estimates, using the Hall (2021) three-dimensional N_c method as summarized in equations (N-5) and (N-6) above.)

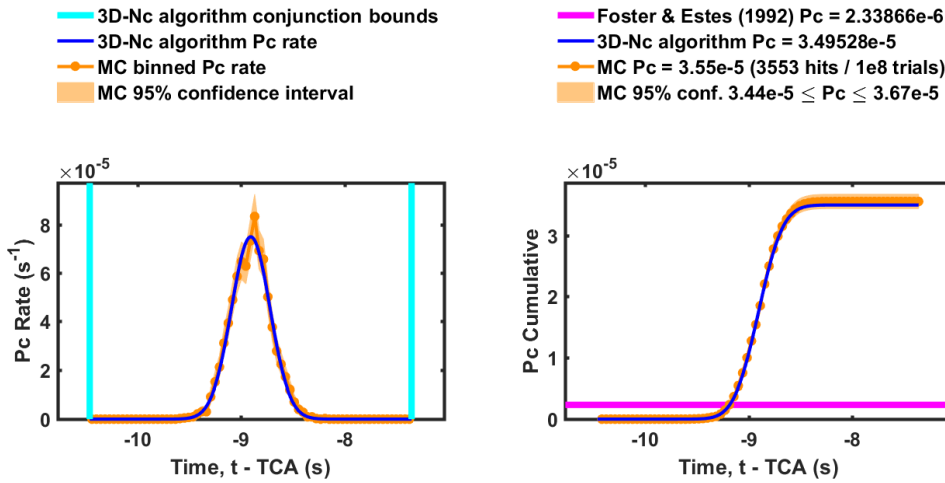


Figure N-5 Pc Rate and Cumulative Pc for a Non-Rectilinear Conjunction

Figure N-5 shows the time-dependent collision rate (left) and the cumulative P_c (right) calculated using the three-dimensional N_c method, as applied to an archived CARA conjunction that has a high relative velocity (~ 13 km/s), but that fails to satisfy the rectilinear motion and Gaussian PDF assumptions. This specific event does not satisfy these assumptions because it involves an object in a highly eccentric orbit with a conjunction occurring in the relatively tightly curved part of the trajectory near perigee, a phenomenology discussed by Hall (2018). In this case, the three-dimensional N_c method calculates a P_c value which accurately matches the Monte Carlo from TCA method P_c estimate, but that is a factor of fifteen larger than the erroneous conjunction plane P_c estimate, calculated in this case using the two-dimensional Foster and Estes (1992) method. It is of interest that the peak point of risk accumulation occurs nine seconds before the TCA, with essentially all the risk accumulated by 8 seconds before TCA. Such a result can seem counterintuitive at first, for one would initially expect that the point of highest risk would always be at the TCA. However, what is operative is the alignment between the geometric miss distance and the covariance. If at TCA very little of the position uncertainty lies along the relative miss vector, then that miss vector is a strong statement of the actual miss; and if the vector is somewhat larger than the hard-body radius (HBR), then the collision risk at that point is quite low. If, however, somewhat earlier or later than TCA the combined covariance (which, it must be remembered, is constantly changing position) does more substantially align along the miss vector, then more possible instantiations of the true miss are likely to be smaller than the HBR (even with the nominal miss vector larger than the expected miss at TCA), so the risk at that point is actually higher. In the more extreme cases, such as that shown in the above example (and even more strongly in the one below), most of the risk accumulation can be relatively far from TCA, meaning that methods that examine the situation only at TCA can misrepresent this risk.

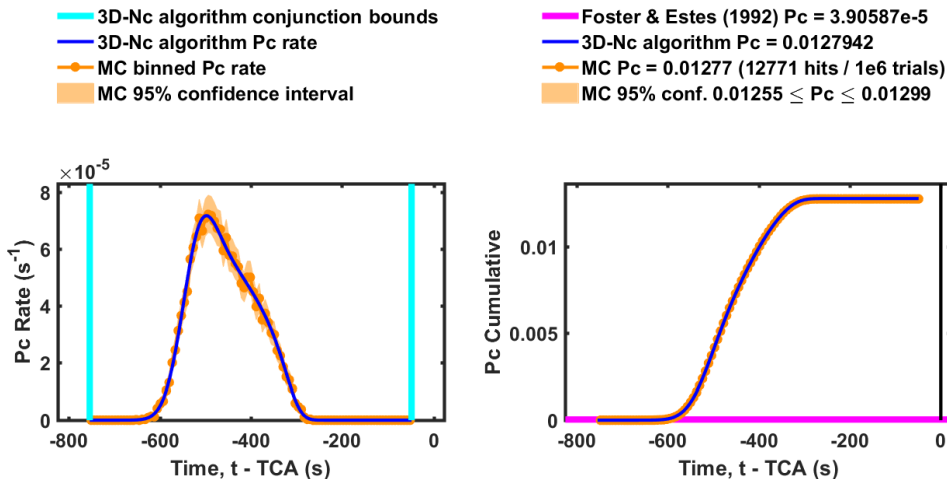


Figure N-6 Pc Rate and Cumulative Pc for a Low Velocity Conjunction

Figure N-6 shows the collision rate (left) and the cumulative P_c (right) for low relative velocity conjunction (~ 3 m/s), that fails to satisfy the rectilinear motion, temporally isolated, and Gaussian PDF assumptions. In this case, the three-dimensional Nc algorithm estimates a P_c value which matches the Monte Carlo from TCA method P_c estimate, but that is a factor of 330 larger than the erroneous conjunction plane P_c estimate.

N.4 Two-dimensional Nc Method Analytic P_c Calculations

As formulated in equations (N-5) and (N-6), the three-dimensional Nc method requires the computation of a time-series of many unit-sphere integrations, each calculated using Lebedev quadrature. However, for temporally isolated conjunctions (i.e., those that are not “extended” or “blended” in time as described by Hall 2021), the integration over time can be approximated analytically, ultimately yielding a single unit-sphere integral. This relatively efficient “two-dimensional Nc” method yields accurate P_c estimates for high velocity, temporally isolated conjunctions (such as the example shown in Figure N-5). However, it is not applicable to low velocity events that are temporally extended or blended (as shown in Figure N-6); these conjunctions still require the use of the three-dimensional Nc method or Monte Carlo estimation.

The first step in the “two-dimensional Nc” formulation involves rewriting the MVN function in (N-6) in the following form

$$MVN(R\hat{\mathbf{r}}, \check{\mathbf{r}}_t, \tilde{\mathbf{A}}_t) = (2\pi)^{-3/2} e^{-Q_{R,t}/2} \quad (\text{N-7})$$

with

$$Q_{R,t} = Q_{R,t}(\hat{\mathbf{r}}) = (R\hat{\mathbf{r}} - \check{\mathbf{r}}_t)^T [\tilde{\mathbf{A}}_t^{-1}] (R\hat{\mathbf{r}} - \check{\mathbf{r}}_t) + \ln(|\tilde{\mathbf{A}}_t|) \quad (\text{N-8})$$

The first term of the $Q_{R,t}$ expression corresponds to an effective Mahalanobis distance that accounts for curvilinear trajectory effects, a function which typically experiences a minimum in time near (but not exactly at) TCA. The second term typically varies slowly in time relative to the first. The next step of the derivation entails numerically finding the minimum of the function



$Q_{0,t}$ (i.e., the function $Q_{R,t}$ evaluated at $R = 0$, which corresponds to the center of the collision sphere) and denotes the time that this minimum occurs as T . In other words, $T = \text{argmin}(Q_{0,t})$. For high velocity conjunctions, this time usually occurs within a few seconds of the TCA (and often much less). The next step is to expand the function $Q_{R,t}$ to second order about the time T , yielding the simplified approximation

$$Q_{R,t} \approx Q_{R,T_*} + \left(\frac{t - T_*}{\sigma_{R,T}} \right)^2 \quad \text{with} \quad T_* = T - \dot{Q}_{R,T}/\ddot{Q}_{R,T} \quad (\text{N-9})$$

and

$$Q_{R,T_*} = Q_{R,T} - \frac{\dot{Q}_{R,T}^2}{2\ddot{Q}_{R,T}} \quad \text{and} \quad \sigma_{R,T}^2 = \frac{2}{\ddot{Q}_{R,T}} \quad (\text{N-10})$$

For this, the required time derivatives $\dot{Q}_{R,T}$ and $\ddot{Q}_{R,T}$ are estimated numerically using finite difference equations (Press et al., 1989). Note, for brevity, the functional dependence on \hat{r} has been suppressed for all of the quantities expressed in equations (N-9) and (N-10). Combining equations (N-5) through (N-10) allows the time integral to be evaluated analytically, and yields the following approximation for a temporally isolated conjunction's statistically expected number of collisions:

$$N_c \approx \frac{R^2}{2\pi} \int_0^{2\pi} \int_0^\pi [v_T \sigma_{R,T} e^{-Q_{R,T_*}/2}] \sin(\theta) d\theta d\varphi \quad (\text{N-11})$$

The integrand depends on the quantities v_T , $\sigma_{R,T}$, and Q_{R,T_*} , each of which is a function of \hat{r} , which in turn depends on the angles φ and θ . Equation (N-10) entails two-dimensional numerical integration over the unit sphere, calculated using Lebedev quadrature. (The function *Pc2D_Hall* of the NASA CARA SDK repository computes Pc estimates for temporally isolated conjunctions using the two-dimensional Nc method.)

N.5 Comparison of Pc Estimates for Temporally Isolated Conjunctions

Figure N-7 shows a comparison of collision probabilities for 63,603 temporally isolated conjunctions extracted from the NASA CARA database for the period 2017-05-01 and 2019-08-15 and for events with $2D P_c > 10^{-7}$ (Hall, 2021). The vertical axes on all three panels plot Monte Carlo (MC) estimates for the collision probability—specifically, Monte Carlo from TCA method Pc estimates, which are also referred to in this figure as two-body Monte Carlo method Pc estimates (i.e., TBMC-Pc estimates, as described in more detail in section N.13). The error bars in Figure N-7 show 95% confidence intervals estimated using the Clopper-Pearson method (1934); several of the conjunctions had zero hits registered in the Monte Carlo simulations, which are represented in Figure N-7 using downward-pointing triangles and a single-sided error bar. The horizontal axes plot the corresponding semi-analytical approximations: two-dimensional Pc on the left graph, three-dimensional Nc in the center, and two-dimensional Nc on the right. The colored points on each plot indicate the results of a



binomial proportion statistical test that evaluates the agreement between the estimates. Specifically, black points in Figure N-7 indicate analytical P_c estimates that agree reasonably well with the Monte Carlo estimates as they do not violate a null-hypothesis that the two are equal at a p -value $\leq 10^{-3}$ significance level. However, those highlighted in yellow do violate the hypothesis at this significance level, and those in red at a more stringent level of p -value $\leq 10^{-6}$. Overall, the two-dimensional conjunction plane P_c comparison plotted in the left graph contains 254 yellow and 436 red points, which both significantly exceed the number of disagreements expected from purely statistical variations, even though together they represent a small fraction (~1%) of the original conjunctions. These disagreements represent conjunctions that violate one or more of the assumptions required for conjunction plane P_c estimation. The center graph clearly shows that the three-dimensional N_c method matches the Monte Carlo P_c estimates better, producing only 66 yellow and zero red points. Finally, the two-dimensional N_c method plotted on the right produces very nearly the same results as the three-dimensional N_c method but requires much less computation time. The three comparisons shown in Figure N-7 indicate that, for temporally isolated conjunctions, the two- and three-dimensional N_c methods are consistent with one another and match Monte Carlo P_c estimates significantly better than the conjunction plane P_c estimation method.

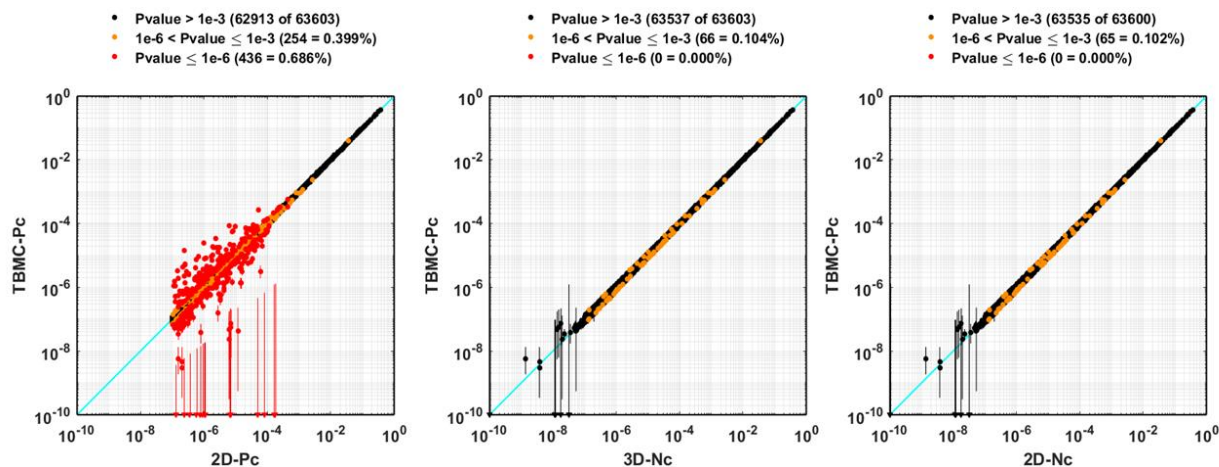


Figure N-7 Comparison of Monte Carlo Collision Probabilities with the Two-Dimensional P_c Method (left), the Three-Dimensional N_c Method (center), and the Two-Dimensional N_c Method (right) for a Large Set of CARA Conjunctions

N.6 P_c Calculations for Multi-encounter Interactions

An additional feature of the two- and three-dimensional N_c methods is their ability to address explicitly the amalgamated risk of repeating conjunctions. While most conjunctions are temporally isolated, there are two conjunction types that exhibit different behaviors. The first type is produced by objects in orbits in synodic alignment that generate a temporal sequence of conjunctions once every revolution or multiple of a revolution (e.g., two nearly circular orbits at different inclinations that produce conjunctions at one or both nodal crossing points). The second type involves objects that orbit close to each other for extended periods, generating extended



interactions with multiple close approaches (e.g., two satellites in nearly the same orbit, but with only a slight difference in inclination and/or eccentricity). In both cases, if each of the multiple encounters is considered separately, situations can arise in which each encounter in the series falls below a P_c mitigation threshold, but the combined risk of all of the encounters exceeds that threshold. The two- and three-dimensional N_c methods account for such multi-encounter interactions by providing estimates for the total expected number of collisions, and upper and lower bounds for the probability of collision (Hall, 2021). The total statistically expected number of collisions for a multi-encounter interaction is given by a summation of N_c values for each conjunction in the sequence

$$N_c(\tau_a, \tau_b) = \sum_{k=1}^K N_{c,k} \quad (\text{N-12})$$

with the index $k = 1 \dots K$ indicating the close approaches applicable to the risk assessment interval $\tau_a \leq t < \tau_b$, and $N_{c,k}$ representing the associated expected number of collisions for each. The upper and lower P_c bounds for the combined interaction are given by

$$\max(N_{c,k}) \leq P_c(\tau_a, \tau_b) \leq 1 - \prod_{k=1}^K (1 - N_{c,k}) \quad (\text{N-13})$$

which also implies that $P_c(\tau_a, \tau_b) \leq N_c(\tau_a, \tau_b)$. Figure N-8 shows an example of a multi-encounter interaction, in which a pair of satellites experience four conjunction events over about a five-hour period. Each of the individual conjunctions produces a P_c value in the upper yellow region (between 10^{-5} and 10^{-4}), as plotted in the bottom panel. The solid line in the top panel shows the upper limit of the cumulative P_c for the interaction; notably, after the third conjunction, the cumulative P_c exceeds 10^{-4} — a value frequently selected as a risk mitigation threshold. So, while these events would not necessarily prompt a mitigation action if examined individually, when considered collectively they do appear to represent a situation of sufficiently high collision likelihood to warrant mitigation. In such a case, it is advisable to run a Monte Carlo investigation (discussed in a subsequent section of this appendix) to verify that the upper-limit P_c value generated by the method is in fact representative of the actual cumulative risk. The utility of the analytic calculation, however, should be clear: if the upper-bound calculation for repeating events is found to be below the mitigation threshold, then there is no need to marshal computationally intensive methods (such as Monte Carlo), for it has already been demonstrated no mitigation action is warranted.

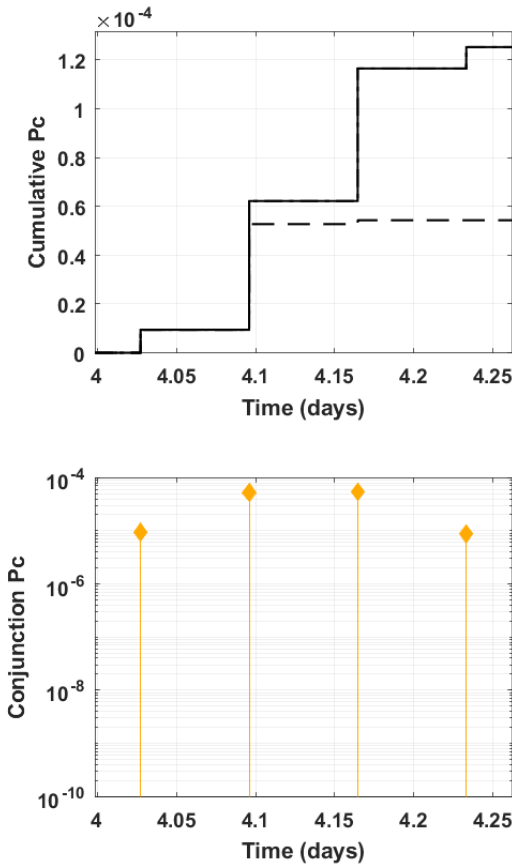


Figure N-8 Cumulative Three-Dimensional N_c Risk Over Four Repeating Conjunctions

N.7 Input Covariance Data Considerations

Most calculations are only as good as the input data that drive them, and P_c calculation is no exception. Appendix P discusses orbit determination quality and propagation issues for individual objects and addresses the question of the circumstances under which the state estimate and covariance might be considered sufficiently poor so as not to constitute a basis for conjunction risk mitigation actions. The purpose of this section is to address the routine improvement and basic error checking extended to covariances as part of the P_c calculation. These activities fall into three basic groups: correction for known problems in propagation, covariance formation and stability issues, and correlation between primary and secondary covariances. Each of these topics will be treated in turn.

N.7.1 Propagation Error Compensation

Historically, accuracy analysis of state estimate and uncertainty estimates has focused on products that emerge directly from the orbit determination fit. These direct orbit-determination products include best-estimate states and covariances of the satellite at an epoch that usually



coincides with the acquisition time of the last tracking metric observation incorporated into the analysis. While these direct orbit-determination products are of course foundational, it is important to remember that most SSA activities, and conjunction assessment in particular, are not usually conducted with these direct products but rather with predictions propagated from the orbit-determination epoch solution, often over a non-trivial duration that spans many orbital revolutions into the future. The batch orbit-determination analysis method used by the DOD produces a formation covariance that represents the expected at-epoch state uncertainty based on the number, quantity, and temporal spacing of the incorporated metric observations; when the state is propagated forward, a parallel process can also be used to propagate the covariance forward in time. The same dynamical models used for the orbit-determination analysis as well as the state propagation itself are used to perform this covariance propagation, although in a linearized way. This means that the propagated covariance will be sized (mostly) appropriately for both the propagation duration and the final prediction point in the orbit.

Despite the use of appropriate models to propagate the covariance forward in time, a number of additional sources of error manifest themselves during the propagation interval yet are not part of the dynamical model used during the fit; these errors are therefore neither incorporated into the orbit-determination-produced covariance nor added as part of the regular propagation process. Because of the prevalence of such outside-of-model errors, techniques have been developed to account for them, the most familiar of which is the addition of process noise during propagation. Originally developed to account for acceleration errors that, due to model inadequacy, were to some degree known, this method propagates a noise matrix alongside the propagated covariance and combines both matrices as part of the overall process. The result is a covariance that is larger than it would have been otherwise to account for these (characterized) errors in the force model(s). A second approach, which is the one used by DOD in the propagation of their orbit prediction products, applies parameters to the covariance before propagation to guide the propagation process in producing a more realistic result. Because this is the approach reflected in the CDM covariances that conjunction assessment practitioners receive from the DOD, it will be described here in some detail.

Orbit determination makes a distinction between “solved-for” parameters that are actually estimated during an orbit-determination activity, and “consider” parameters that are not “solved for” but represent *a priori* information that is “considered” as part of the orbit-determination process. In the present case, the use of the term “consider parameter” is somewhat non-nominal in that it is referring not to additions or alterations made during the fit but to modifications to the fit-produced covariance so that when it is propagated, it may give a more realistic representation of the expected state errors. For DOD covariances, two different consider parameters are applied to compensate for two distinct expected errors during propagation: atmospheric density forecast error and satellite frontal area uncertainty.

Atmospheric drag is a significant force that affects satellite orbits with perigee heights less than 1000 km, and the calculation of the expected atmospheric drag at any particular moment requires an estimate of the neutral atmospheric density that that satellite will encounter at that moment. Because the atmospheric models that generate this estimate are driven by space weather indices, the ability to predict these indices accurately affects the fidelity of the predicted atmospheric



density and thus the atmospheric drag. Unfortunately, it is difficult to predict future space weather indices well, primarily because they are affected by activities on the part of the sun's surface that has not yet rotated into view from the Earth. This particular issue was studied with the Jacchia-Bowman High Accuracy Satellite Drag Model (HASDM) 2009, which is the atmospheric density model used by DOD, by comparing predicted densities (using predicted space weather indices) to actual densities and producing polynomial fits of the relative density error as a function of satellite perigee height and the Ap (major magnetic storms list) and Dst (disturbance storm-time) space weather indices. Figure N-9 shows the behavior of these polynomial fits divided into four different classes of Ap/Dst activity; y-axis values are omitted here to allow full releasability of the figure:

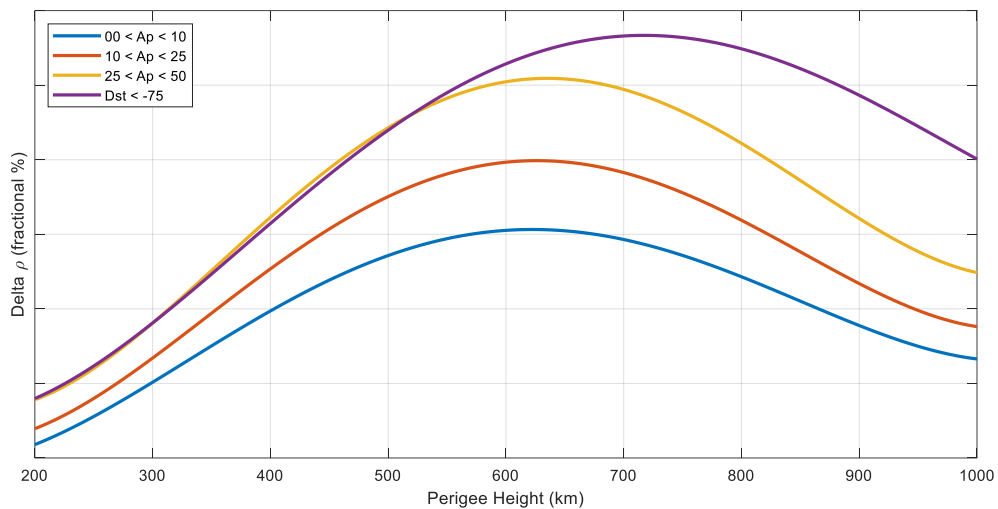


Figure N-9 Behavior of Relative Density Error by Perigee Height and Solar Activity

These fits produce a variance term that can be added to the ballistic coefficient variance in the covariance: because in the drag equation the ballistic coefficient and the atmospheric density estimate are multiplicatively coupled, changing one of these parameters has the same effect as changing the other. When the covariance is propagated, this augmented term will appropriately expand the other covariance terms.

The amount of drag acceleration a satellite encounters is also governed by the frontal area that the satellite presents to the atmosphere; this makes intuitive sense (amount of resistance is a function of area presented to the resisting fluid) and is reflected in the ballistic coefficient (B) equation

$$B = C_D \frac{A}{M} \quad (\text{N-14})$$

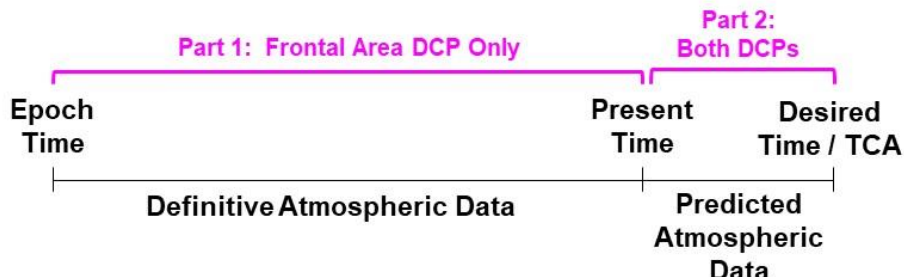
in which C_D is the (dimensionless) drag coefficient, which indicates the degree to which the satellite surface is susceptible to drag resistance; M is the satellite mass; and A is the satellite frontal area. As A increases, B increases as well, increasing the overall drag acceleration value.



Stabilized satellites should manifest a stable B term, but rotating satellites, because their frontal area term is continuously changing, can exhibit a range of B terms. Three outcomes are possible depending on the rapidity of the rotation: the effect can be washed out during the fit (because the rotation is so rapid that an average value is quite representative), the effect can be not relevant during the fit (because the rotation is so slow that it does not affect near-term look-back and look-forward), or the effect can be such that the rotation does affect results fit-to-fit. It is this last case for which compensation is helpful. A history of regularized B histories for individual satellites is examined and a relative error and variance calculated, and this variance is added to the drag variance in the covariance as a corrective term whose influence will be realized in propagation.

There is some additional subtlety regarding the exact way these consider parameters are applied. A typical propagation consists of two conceptual stages: the first stage is the propagation forward from the epoch time of the orbit determination to the present time, which can make use of measured and thus highly reliable space weather indices; and the second stage is from the present time to the desired final propagation time, which has to use predicted space weather indices and the errors that these introduce. The two consider parameters are thus applied at different times. Because satellite rotation and its resultant uncertainty will occur for the entire interval from epoch time to the propagation end point, that consider parameter is applied at epoch.

Atmospheric density forecast error, however, is encountered only forward in time from the present moment, so it is added only for that portion of the propagation. Figure N-10 outlines the two-phase application of these consider parameters:



DCP = Dynamic Consider Parameter

Figure N-10 Two-phase Application of Consider Parameters

If the CDMs generated by the DOD are used for conjunction assessment applications, the good news is that all the consider parameter activities described above are already performed—the propagated covariances that the CDM contains have had these two consider parameters applied during the covariance propagation executed at the DOD work center. If one is working with epoch state estimates, which is sometimes necessary when performing P_c calculations with Monte Carlo techniques, then manual application of the consider parameters may be necessary. This issue is discussed at greater length in the section that addresses Monte Carlo P_c calculations.



N.7.2 Defective Covariances

There are several ways in which a covariance contained in a CDM can be defective.

- **Null Covariances.** All-zero, or null, covariances are sometimes observed, usually arising from a conjunction assessment screening for which the O/O-provided ephemeris does not contain covariance data. In such a case, it is possible to compute the P_c either using only the one covariance that the CDM message contains or by applying a special technique that determines the maximum P_c possible presuming that the null covariance could take on any possible value (developed and described in Frisbee 2015).
- **Default Covariances.** Default covariances are diagonal covariances that contain a value of ten earth radii squared for each of the three position variances. The presence of this covariance indicates that a precision, special-perturbation solution for the object was not possible; the state estimate provided arose from a general-perturbation solution, and an orbit-determination-produced covariance was not available. Such a result is not a precision solution and does not constitute a basis for conjunction risk mitigation actions.
- **Non-Positive-Semidefinite Covariances.** Another defective covariance type found in CDMs, now quite rare due to improvements to the DOD operational system, is a covariance that fails to be positive semidefinite. A positive semidefinite matrix is one that contains no negative eigenvalues. Because the covariance represents a hyperellipsoid of actual state error information, it must have a set of eigenvalues all greater than or equal to zero for error information to consist of real rather than imaginary quantities. The orbit-determination mechanism that generates the covariance should always produce at least a positive semidefinite matrix, for the linear algebra function involves the product of a square matrix and its transpose, and one can prove that this procedure always produces a positive semidefinite result. Due to either numerical precision limits or interpolation, the provided matrix is sometimes not positive semidefinite. If the 2×2 projection of the covariance matrix into the conjunction plane is not positive semidefinite, the two-dimensional P_c calculation is not possible. If the full 6×6 or 8×8 matrix is not positive semidefinite, then Monte Carlo sampling on the entire matrix is not possible either.

As such, some attention must be paid to this issue of positive semidefinite matrix conditioning. A recent paper on this subject (Hall 2017b) examined the issue in some detail and compared different matrix repair algorithms to minimally adjust the covariance to make it positive semidefinite compliant; it found that most repair approaches yield equivalent answers in terms of the resultant calculated P_c . An “eigenvalue clipping” procedure was developed in which any negative eigenvalues (which are almost always small) are set to a small positive or zero value, as required.

The CARA operational implementation of this method proceeds parsimoniously, namely by directing such repair only to the level needed to perform a calculation. For example, a covariance used for the two-dimensional P_c calculation would neither be tested for positive semidefinite compliance in its full 8×8 form nor its position-only 3×3 form; instead, the 2×2 projection of the joint covariance into the conjunction plane would be tested and repaired only when necessary.



to enable the two-dimensional P_c calculation. To do otherwise is to make repairs and potentially alter the result when this is not strictly necessary.

The P_c Computation CARA SDK includes the source code for identifying the need for and making the covariance matrix repairs described above; it is available in the NASA CARA software repository. (See Section 7, Contact Information in this document for the specific URL.)

N.7.3 Covariance Correlation

For nearly all the broader conjunction assessment conduct during the past decade, practitioners operated with the presumption that the primary and secondary objects' covariances could be considered uncorrelated. Not only was this the "right" answer in that it greatly simplified the P_c computation because the joint covariance could be formed by simple addition of the two covariances, but there was also a good intuitive justification for the presumption. Because the focus had been on the two objects' orbit-determination fits, which are based on separate sets of observations, there was no expectation that there would exist any significant correlation between the two objects' covariances. The principal source of potentially correlated error was presumed to be uncharacterized but correlated errors in space sensor observations used by both primary and secondary objects. Because most primaries receive many observations from many different sensors, it was seen as unlikely that this particular source would introduce much correlation. Correlation between covariances was thus expected to be small, and conjunction assessment operators proceeded as though it were.

With the initiative several years ago to include outside-of-fit prediction error characterization into DOD satellite covariances (see the above section on Propagation Error Compensation), the issue of covariance cross-correlation began to be rethought. The principal outside-of-fit prediction error is global atmospheric density forecast error due to inadequate space weather index prediction. Because this is a global error, it is likely to be shared among large classes of objects, some of which might constitute both the primary and secondary objects in a conjunction. As discussed previously, this global density forecast error has been parameterized by satellite perigee height and predicted geomagnetic index, so the degree of such error, both identified separately and injected into each DOD-furnished covariance by means of a consider parameter, is known for each satellite. It is possible to determine the degree of shared error from this source and account for it when forming the joint covariance.

A study by Casali et al. (2018) provides a full development of this theory and presents results for an evaluation set of conjunction data. Essentially, one has to determine the global density forecast error relevant to each satellite and the degree to which the associated drag error induced by this density forecast error will manifest itself in position error relevant to the particular conjunction. The governing equation is the following:

$$P_m = P_s + P_p - \sigma_{s/g} \sigma_{p/g} G_s G_p^T - \sigma_{s/g} \sigma_{p/g} G_p G_s^T \quad (N-15)$$

in which P_m is the decorrelated joint covariance at TCA, P_s is the secondary covariance at TCA, P_p is the primary covariance at TCA, $\sigma_{s/g}$ is the density forecast error germane to the secondary satellite, $\sigma_{p/g}$ is the density forecast error germane to the primary satellite, G_s is the sensitivity vector mapping drag acceleration error to secondary satellite position error at TCA, and G_p is the



sensitivity vector mapping drag acceleration error to primary satellite position error at TCA. One could wonder how the conjunction assessment practitioner would come upon all of the needed data to effect the proposed compensation. A recent enhancement to the DOD operational system has placed all of this information in the CDM itself, allowing the direct calculation of the decorrelated joint covariance. The CARA Pc Calculation SDK, available on the NASA CARA software repository, contains both a math specification outlining this calculation and source code to perform it. (See Section 7, Contact Information in this document for the URL.) Hall (2021) describes how the density forecast errors and sensitivity vectors can be used to estimate decorrelated joint covariances for the two- and three-dimensional Nc methods.

A heuristic probing of the situation reveals that, conjunction by conjunction, different levels of P_c changes are possible due to cross-correlation remediation. Orbits that are insensitive to atmospheric drag are little affected by density forecast error and will have P_c estimates that, as expected, also change little. Head-on conjunctions are expected to be left mostly unaffected as well, for the components of the error that govern the P_c are not subject to density forecast error perturbation. Crossing events are perhaps the most susceptible to cross-correlation effects, especially if the drag level of both satellites is similar.

The plot in Figure N-11 profiles 250 conjunctions in which the primary and secondary satellites are of non-negligible drag (i.e., Energy Dissipation Rate (EDR) values greater than 0.0006 watts/kg; see Hejduk 2008 for an explanation of energy dissipation rate) and plots the ratio of the P_c calculated with the decorrelated joint covariance to that of the P_c calculated with the unmodified joint covariance. One can see that for somewhat more than half of the events, the ratio hovers near unity, meaning that the conjunction is little affected by the compensation. For about one-third of the cases, the decrease in P_c is notable, in many instances more than an order of magnitude. For the remaining cases, there is an increase in P_c from a factor of 1.5 to 5.

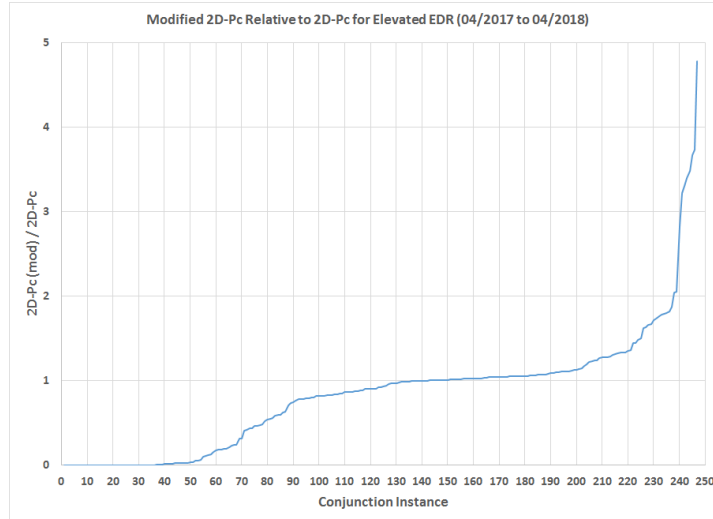


Figure N-11 Profiles of 250 Conjunctions with Primary and Secondary Satellites of Non-negligible Drag¹⁴

While the P_c value changes by less than a factor of 1.5 for most of the conjunctions, a sufficient number are affected more substantially therefore justifying the integration of this additional consideration into the P_c computation, especially because it is a straightforward calculation from data provided directly in the CDM.

N.8 Monte Carlo P_c Calculation Techniques

Analytic approaches to P_c calculation are more computationally efficient than Monte Carlo methods, especially the conjunction plane two-dimensional P_c method. However, as discussed previously, analytic methods require certain enabling assumptions that are not necessarily valid for all conjunctions. Monte Carlo approaches require fewer enabling assumptions, but they are not typically employed as the first method of computation. Instead, Monte Carlo methods are usually reserved for cases that are suspected of violating the enabling assumptions of the analytic methods. As described by Hall et al. (2018) and Hall (2021), there are two strains of the Monte Carlo method that are regularly employed:

- “Monte Carlo from epoch,” in which the orbit-determination-epoch mean states and covariances are used to generate sampled states, and potentially long (i.e., multiday) high-fidelity propagations are required for each Monte Carlo trial.
- “Monte Carlo from TCA,” in which the mean states and covariances predicted at TCA are used to generate sampled states, and only relatively short propagations to each trial’s new TCA are required.

Each of these two approaches will be discussed in turn.

N.8.1 Monte Carlo from Epoch

¹⁴ From Casali et al. 2018.



The principal appeal of calculating the P_c using the Monte Carlo from epoch approach is that it requires almost no simplifying or restrictive assumptions, making it as close to a “gold standard” for P_c estimation as can be devised. The input information includes the states and covariances for the primary and secondary objects at their respective orbit-determination epoch times, the combined hard-body radius of the two objects, and an ensemble of environmental datasets required for the high-fidelity propagations (such as predicted space weather indices and atmospheric density debiasing data; see Hall et al. 2018). The most elaborate instantiation of this technique uses the full eight-dimensional orbital state vectors (each containing six coordinate or element variables, plus drag and solar radiation pressure variables) along with the associated 8x8 covariance matrices for the primary and secondary satellites.

For each Monte Carlo trial, a state perturbation is obtained by performing a random draw from the distribution using the covariance matrix to generate the associated Gaussian distribution for each variable. These perturbations are then used to alter the initial states by adding each to the appropriate epoch mean state estimates. To do this for the primary satellite, for example, one would generate random perturbations for the eight variables representing the primary satellite’s state based on their distribution as defined by the covariance, and then create a new, sampled state vector by adding the (signed) perturbations to the mean epoch state vector. This same procedure would also be performed for the secondary satellite. This sampling process generates epoch states for both the primary and secondary objects that represent statistically reasonable alternatives for their actual states. These two sampled epoch states are then propagated forward, a TCA identified, and a check performed to determine whether the miss distance at TCA is smaller than the hard-body radius; if it is, the trial results in a simulated collision and a “hit” is registered; if not, it is considered a “miss.” This sampling/ propagation/ hit-registration procedure is then repeated for a large number of Monte Carlo trials, and the final number of hits divided by the total number of trials constitutes the Monte Carlo P_c estimate. There are algorithms that can be applied to estimate the confidence interval on the Monte Carlo P_c after a given number of trials due to event counting uncertainties (e.g., MATLAB’s *binofit* function).

This procedure seems straightforward enough, and in many respects it is. But there are subtleties that require attention, especially if the technique is deployed for LEO conjunctions:

- For the result to be valid, the same force models and force model settings must be used for the Monte Carlo propagations as were used when generating the original orbit-determination solution. While it often is not difficult to apply the same general force model settings, there does need to be overall compatibility between the orbit-determination engine and the Monte Carlo propagator, such as the same set of geopotential Legendre polynomial coefficients (not just the same geopotential order) and, most critically for LEO, the same atmospheric density model. While it may be possible to deviate somewhat from this level of compatibility and still obtain reasonably accurate outcomes, the “gold standard” propriety of the result is lost.
- Correlation between the primary and secondary covariances, as described in the previous section, should be considered. This correlation can be modeled during the random draw process by forcing correlation in the primary and secondary objects’ drag perturbations.



- Monte Carlo from epoch often requires extremely long computation run times. The run time is a function of the actual P_c , since this will determine how often hits are likely to occur and the number of trials required to obtain a result with a desired confidence level. Without marshalling extensive high-performance computing, the P_c levels that can be explored with this method have to remain relatively large (e.g., 10^{-5} or above). Computation times for smaller P_c events can be prohibitively long. For example, validating a P_c estimate of $\sim 10^{-7}$ at the 95% confidence level for a conjunction with TCA five days from the orbit determination epoch time would require an estimated two years of execution time on a 20-CPU, reasonably modern server (Hall et al. 2018). For this reason, it is typically necessary to reserve the Monte Carlo from epoch method for larger P_c events only, which means that one must trust analytic methods to identify a candidate subset of conjunctions for follow-up Monte Carlo analysis.
- High-fidelity orbital state propagations require the most processing during typical Monte Carlo from epoch computations, so when applying this approach, there is a temptation to “reuse” propagations to gain computational efficiency. Suppose that ten perturbations were performed for the primary satellite and ten propagated ephemerides were generated, and the same was done for the secondary object as well. Ephemeris #1 for the primary could be compared to ephemeris #1 for the secondary to determine whether a hit occurred, ephemeris #2 for the primary to ephemeris #2 for the secondary, ephemeris #3 for the primary to ephemeris #3 for the secondary, etc., and have as a result ten comparisons/trials. To go further, one could compare ephemeris #1 for the primary to ephemeris #2 for the secondary, ephemeris #1 for the primary to ephemeris #3 for the secondary, etc., and realize 100 comparisons/trials from merely 20 total propagations. Such a procedure certainty seems advantageous, given that processing time is the limiting factor to the deployment of Monte Carlo from epoch, and following such a procedure will produce a result that converges on the true P_c . The drawback is that such reuse of samples violates the conditions for the proper application of the formulae to calculate P_c uncertainty confidence intervals. Monte Carlo results without associated reliable confidence intervals are not operationally useful because it is never known how close one is to the true P_c value. Schilling et al. (2016) discuss this issue and confirm it to be a problem, and they recommend some estimation techniques that allow (large) confidence intervals to be constructed around Monte Carlo products that avail themselves of sample reuse. The CARA implementation has avoided any such sample reuse to ensure that the “gold standard” status of the results not be in question and to produce more narrow confidence intervals.

Due to all the above considerations, but especially the run-time requirements, Monte Carlo from epoch is usually reserved only for those cases that require it for accurate P_c estimation.

A study effort discussed in greater detail in the next section determined that the Monte Carlo from epoch method appears to be needed only when the two objects stay in such close proximity that they experience a sequence of multiple, comparable-risk close approaches during a multiday risk assessment projection interval. For closely spaced co-orbiting objects, these conjunctions may also become effectively “blended” in time with one another such that collision probability



accumulates appreciably even during the mid-point times between the encounters rather than just during short bursts very near the close approaches (Baars et al. 2019). In such cases, two impediments arise to estimating accurate P_c values using methods formulated for temporally isolated close approaches. First, there is no clear, single TCA at which to evaluate the collision likelihood. While one could in fact find the unique point of closest approach between the two nominal trajectories for the entire sequence and perform a two-dimensional P_c calculation for that encounter, there is no guarantee that another encounter in the sequence may actually possess a higher P_c due to different covariance orientations even though it has a larger nominal miss distance. Second, calculating a single encounter P_c at each of the close approaches and then amalgamating these using the following formula (derived from DeMorgan's Law of Complements)

$$P_{Tot} = 1 - \prod_{i=1}^n (1 - P_{ci}) \quad (\text{N-16})$$

potentially overestimates the overall collision likelihood because it presumes that the individual events in the sequence are statistically independent, but in fact they may not be, especially if blended in time. This total probability estimate matches that given in equation (N-13) and provides an upper bound for the amalgamated risk over the time interval of interest. For maximum efficiency, Monte Carlo from epoch would then be run operationally only in cases in which this upper bound is above a mitigation threshold and there is interest in determining whether the higher-fidelity Monte Carlo calculation would reduce this value to one much closer to or below the threshold. Monte Carlo from epoch can also be run if there is any question about the overall rectitude of the P_c calculation. As stated earlier, lower- P_c conjunctions may present intractable Monte Carlo execution times, but if one wishes only to ensure that the Monte Carlo P_c falls below the mitigation threshold (rather than establish a high-fidelity P_c value), this can usually be accomplished with far fewer Monte Carlo trials.

Optimal application of the Monte Carlo from epoch P_c estimation method does not entail P_c evaluation over a relatively short time interval bracketing a single conjunction's TCA, but rather over a more extended interval that spans several close approach encounters. For example, the collision likelihood between two objects would not be evaluated at the nominal TCA for a single conjunction, but, perhaps, over a risk assessment interval projecting forward seven days. This multiday interval would not only include the original nominal TCA but also a sequence of other encounters between the primary and secondary as well. In this case, each Monte Carlo trial would be propagated forward seven days and a hit registered at the earliest time that the hard-body radius is violated, if such a time exists (Hall et al. 2018 and Hall 2021). Temporal risk plots can be produced using the sequence of hits registered during all the trials, an example of which is shown in Figure N-12 (which shows the same conjunction sequence as Figure N-8 from the earlier discussion of two- and three-dimensional N_c calculation methods). The pink shaded area in Figure N-12 shows the Monte Carlo P_c estimation confidence region, and the pink line shows the best estimate Monte Carlo result. As can be seen, the black upper line, which is the upper bound estimate from the three-dimensional N_c function, is within the confidence interval of the Monte Carlo results and thus is a reasonable actual realization of the repeating conjunctions' cumulative risk.

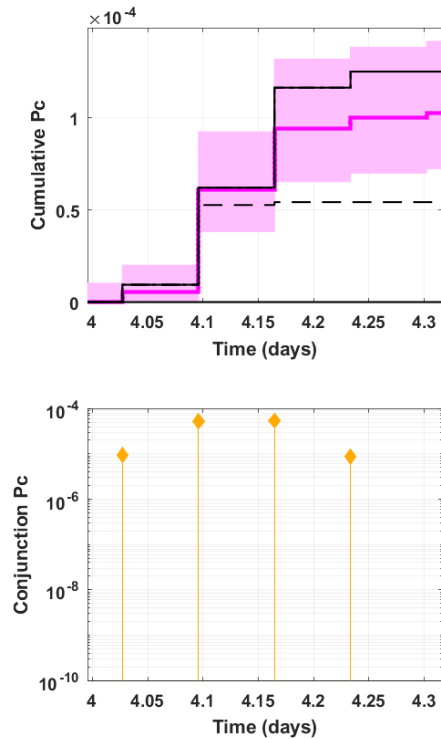


Figure N-12 Three-Dimensional Nc Temporal Risk Plot with Monte Carlo from Epoch Result Overlay (in Pink)

Because it is complicated to set up the execution environment for the Monte Carlo from epoch calculation, and because “gold standard” results require assembling extensive environmental data and software settings identical to the original DOD orbit-determination solutions, it is envisioned that the ability to run this strain of Monte Carlo estimation will remain with NASA CARA. However, a more computationally efficient mode of Monte Carlo estimation, which is serviceable for several different applications and is easier to obtain and employ operationally, is described in the next section.

N.8.2 Monte Carlo from TCA

A much more computationally efficient variant on Monte Carlo from epoch, which has been used by conjunction assessment practitioners for some time, is Monte Carlo conducted from TCA, or two-body Monte Carlo (TBMC)-P_c estimation. As the definition implies, the Monte Carlo simulation begins with the primary and secondary objects’ equinoctial element states propagated to TCA. Perturbation and sampling of both states is conducted much as described earlier for Monte Carlo from epoch, and each sampled primary and secondary state is propagated both forward and backward in time to find the pair’s TCA and determine whether the corresponding miss distance is smaller than the hard-body radius (backward propagations are required to register hits that occur at times before TCA). The simplification arises from the fact that, since one is beginning from TCA, the propagations required will be short. This means that an efficient two-body motion propagation scheme usually provides an accurate trajectory



approximation, and this, combined with the very short propagation times, vastly improves the computational efficiency of the calculation—by a factor of 10,000 to 100,000 according to the study by Hall et al. (2018). This specific method of Monte Carlo from TCA is also referred to as “two-body Monte Carlo” Pc (TBMC-Pc) estimation. To use the TBMC-Pc method, the conjunction duration needs to be short so that one may safely presume a single, unblended event that does not require the Monte Carlo from epoch method. As a second condition, one must have confidence that both objects’ states and covariances propagated to TCA are good representations of the states and state uncertainties at that point. Usually, there is reasonable confidence in the mean state estimates themselves, but the covariances are a different matter: a number of studies (e.g., DeMars et al. 2014) have indicated that propagated covariances represented in Cartesian space fail to represent the actual uncertainty distributions, due both to the potential failure of the linearized dynamics to remain representative over long propagation intervals and, more importantly, a mismatch between elongated in-track uncertainty volumes and the forced representation of these uncertainty volumes as Cartesian ellipsoids. The latter problem is illustrated in Figure N-13. The actual in-track error volume should follow the curved trajectory of the orbit, but the Cartesian covariance is limited to the rectilinear representation shown: as the elongation grows in the in-track direction (which occurs for longer propagations), the mismatch between the two representations also increases.

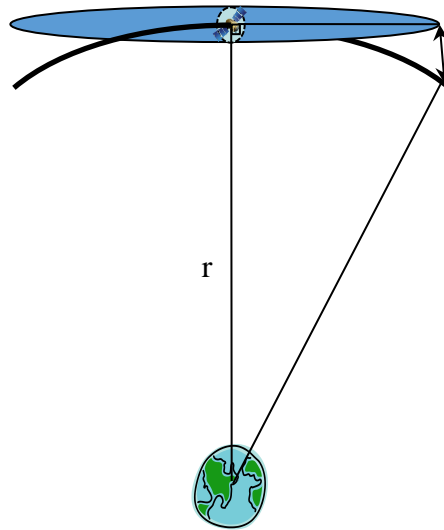


Figure N-13 Mismatch between Elongated In-track Covariances and Forced Cartesian Ellipsoidal Representation

To address the latter problem, the results from a study conducted by Sabol et al. (2010) are both important and extremely helpful. This study addressed directly the question of the optimal choice of orbital state representation for covariances, finding that it is not the specific state representation in which the propagation is executed but rather the one in which the propagated covariance is rendered that ultimately governs the realism of the uncertainty distribution and associated error volume. Specifically, if the covariance is rendered and used in a curvilinear state representation, such as equinoctial elements, then it tends to represent the error volume much more accurately than if it is transformed and used in Cartesian coordinates. The surprising result



is that a non-representative Cartesian covariance transformed into an equinoctial covariance becomes a representative covariance. Furthermore, taking random samples using the equinoctial state representation and performing the non-linear conversion of each sample to Cartesian coordinates generates a point cloud in the Cartesian frame that also approximates the true error volume much more accurately.

This latter procedure allows the Monte Carlo from TCA method to employ more realistic uncertainty volumes, at least with respect to orbital state representation-related mismatches. The detailed procedure is the following:

1. Convert both objects' states and covariances at TCA to equinoctial elements.
2. Generate a set of perturbations for each object based on the equinoctial covariances.
3. Combine these with the mean equinoctial states to generate sampled equinoctial states for the primary and secondary.
4. Convert these sampled states from equinoctial elements to Cartesian coordinates using the non-linear transformation.
5. Propagate the Cartesian states for both the primary and secondary using two-body equations of motion to find the new TCA, which may precede or follow the nominal TCA.
6. Determine whether the new miss distance is less than the hard-body radius, and if so, register a hit at the time that the hard-body radius sphere is violated.
7. Repeat steps 5-6 until the entire set of Monte Carlo sampling trials has been processed.
8. The P_c is the number of hits divided by the total number of trials, and the confidence interval can be calculated from an appropriate formula.

This approach seems reasonable enough; but it would be presumptuous to assert, without further study, that it is truly robust, especially since the question of the durability of the linearized dynamics typically used to propagate covariances was not directly addressed. As it is, additional study efforts have been performed to verify that it is indeed sufficiently representative for conjunction assessment applications, and they are described below.

The first of these study efforts was performed as part of the previously cited analysis by Hall et al. (2018). A set of 373 high- P_c conjunctions was selected and evaluated with both Monte Carlo from epoch and Monte Carlo from TCA, and the comparative results are shown in Figure N-14. The top window is a scatter plot of the P_c calculated by Monte Carlo from epoch versus that from Monte Carlo from TCA. The intersection of each “plus” sign gives the scatter-plot point, and the length of the plus-symbol tails indicates the uncertainty of the calculation. One can see that the agreement is strong because all the points are close to the dashed y-x line that would indicate perfect equality. The bottom window plots the base-ten logarithm of the ratio of P_c values estimated using the Monte Carlo from epoch method to those estimated with the Monte Carlo from TCA method. The largest deviations are about 0.2 of an order of magnitude in P_c , which is considered to be below operational significance. A separate statistical test for similarity of results produced p -values all less than 10^{-3} , indicating that one should reject a hypothesis that



these results arise from different distributions. Good agreement is thus observed between the abbreviated Monte Carlo from TCA and Monte Carlo from epoch results.

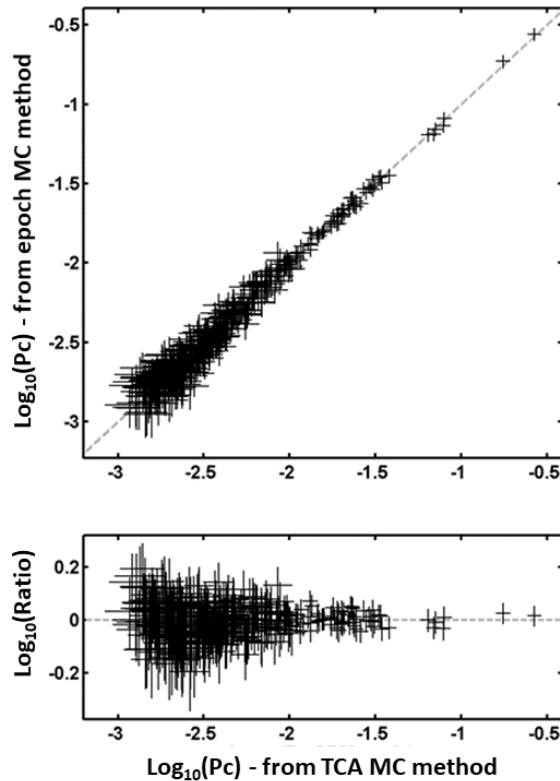


Figure N-14 Comparative Results of 373 High-Pc Conjunctions¹⁵

The second study effort involved a comparison between the Monte Carlo from TCA Pc estimation method and the two-dimensional Pc method (Hall 2019b), which was later extended to compare the from TCA method to two- and three-dimensional Nc methods (Hall 2021). In these studies, 63,603 temporally isolated conjunction events with two-dimensional Pc values greater than 10^{-7} were subjected to Pc calculation by the two-dimensional Pc method, as well as the two- and three-dimensional Nc methods, and all of these were compared to the Monte Carlo from TCA method. The comparative results are shown in Figure N-15 (which refers to Pc values estimated using the Monte Carlo from TCA method as TBMC-Pc values). These plots are similar to those already shown in Figure N-7, except in this case the colored diamonds represent the worst kind of Pc estimation failure, i.e., conjunctions in which the analytical calculations significantly underestimate the Monte Carlo from TCA method Pc values. The left panel shows that, although the two-dimensional Pc method performs reasonably well for the vast majority of temporally isolated conjunctions, it underestimates from TCA Pc values by a factor of 1.5 or more in 0.258% of the investigated cases. (See the top legend of the left graph.) For those cases that showed large disparities, the subset that had true Pc values in the tractable range for Monte Carlo from epoch were validated with this methodology; and in each case the Monte Carlo from

¹⁵ From Hall et al. 2018.



epoch reruns matched the output from the Monte Carlo from TCA. To the degree that non-representative covariances may be responsible for two-dimensional Pc failures (due to coordinate frame mismatches), Monte Carlo from TCA certainly appears to be able to recover the true Pc. As an aside, some of these differences between the conjunction plane two-dimensional Pc estimates and the Monte Carlo method estimates are considerable; there are several cases in which the two-dimensional Pc estimate understates the Monte Carlo from TCA estimate by more than an order of magnitude, as shown in the red in the left panel of Figure N-15. The center and left panels of Figure N-15 show that the three- and two-dimensional Nc methods do not similarly underestimate the from TCA Pc method values, except in a few statistically insignificant cases.

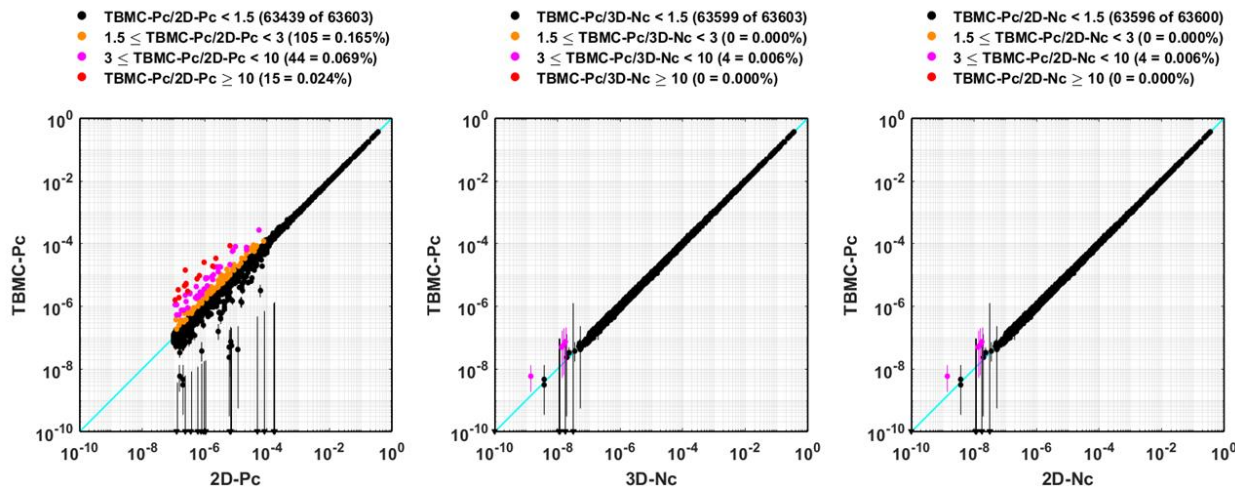


Figure N-15 Comparative Results of 63,603 Conjunction Events¹⁶

Originally, Monte Carlo from TCA was advanced as a robust and computationally tractable way to ensure reliable Pc calculations in the face of occasional miscarriage of the two-dimensional Pc algorithm. However, Figure N-15 demonstrates that the development and testing of the two- and three-dimensional Nc analytic methods have led NASA CARA to recommend that these methods supplant routine use of Monte Carlo from TCA. One may still resort to this more computationally efficient Monte Carlo method if desired, but testing indicates that the Nc calculation methods outperform Monte Carlo from TCA (in that it accurately matches Pc estimates for isolated conjunctions and also provides a cumulative risk upper bound for repeating conjunctions) and is at least an order of magnitude more computationally efficient, especially for events with small Pc values. Monte Carlo from TCA is a capability available for download from the NASA CARA software repository,¹⁷ and O/Os who are currently using it or a similar implementation are not urged to take it out of service, but as a Pc calculation approach, it does not seem to offer any enduring advantage over the two- and three-dimensional Nc methods.

Finally, a dedicated study on covariance Gaussianity was recently conducted (Lechtenberg 2019b). The same set of 44,000 conjunctions used by Hall (2019b) was analyzed for multivariate

¹⁶ From Hall 2019b and Hall 2021.

¹⁷ Specifically, the *MCWorkbench* SDK function estimates TBMC-Pc conjunction values using CDM test files as input. See Section 7, Contact Information in this document for the CARA software repository URL.



normality of the position covariance in Cartesian coordinates. The methodology was to convert the covariance to equinoctial elements, generate a set of random position samples from this covariance, convert the sample set to Cartesian coordinates, and apply a multivariate normality test (here the Henze-Zirkler test) to assess compliance to this distribution. At a 5% significance level, only 60% of the cases could be considered to conform to a multivariate Gaussian distribution in Cartesian coordinates. In principle, such conjunctions would be considered suspect cases whose two-dimensional P_c results would be considered doubtful. As it is, since such a large fraction of the investigated cases show good agreement between the Monte Carlo at TCA and the two-dimensional P_c , clearly the Gaussianity of the covariances in the Cartesian framework does not matter appreciably for the P_c calculation. This result corroborates that of an earlier study by Ghrist and Plakalovic (2012), which reported similar findings.

How can this be, given that the covariance is integral to the two-dimensional P_c calculation? It is important to remember that the analyses above are restricted to high- P_c events. For the probability of collision to be high, significant overlap needs to exist between the primary and secondary object covariances; this means that the central parts of the covariances, which are where most of the probability density lies, have to overlap substantially. Such a requirement makes the behavior of the tails of the covariance much less important, and it is in the tails that non-Gaussian behavior is most strongly manifested. Even though a good number of conjunctions fail tests for covariance Gaussianity in Cartesian coordinates, for high- P_c events, this result does not appear to affect the rectitude of the calculated P_c . A difference probably is observable for lower- P_c conjunctions, but because these conjunctions are not operationally significant, it is not operationally important to identify or characterize this phenomenon.

There is the lingering question of the eventual failure of the linearized dynamics in propagating covariances since DOD covariances are propagated through a pre- and post-multiplication by a linearized state transition matrix. It is agreed that, given sufficiently long propagations, such an eventuality should arise. However, the propagation duration required for this problem to manifest itself substantially is believed to be much longer than encountered for most conjunctions—on the order of weeks. This is why more attention is paid to this phenomenon in other areas of SSA such as uncorrelated track processing for which propagations of 30 days or more may be required, whereas it is rare for propagations longer than ten days to take place in conjunction assessment. Of course, fresh tracking data are always appreciated as they shorten the propagation interval and lend additional confidence to the solution.

N.9 Choosing an Appropriate Hard-Body Radius

As discussed in the first section of this appendix, the hard-body radius represents the combined size of the primary and secondary objects; the word “radius” is used because this combined size is typically envisioned as a sphere, and the radius of a sphere is a convenient linear representation of its size. The hard-body radius is needed for the P_c calculation because it represents the circle/sphere within which a simultaneous penetration by both the primary and secondary objects’ trajectories will constitute a presumed collision. It is not just a required input to the P_c calculation, however, it is also one of the governing parameters of the calculation: the P_c value represents an integral over the area of the hard-body radius circle (or surface area of the hard-body radius sphere) and thus in many circumstances, varies roughly in proportion to the



square of the hard-body radius, so an increase of the hard-body radius by a factor of three increases the calculated P_c by a factor of nine, or nearly one order of magnitude. Because of this sensitivity, it is important not to overstate the hard-body radius simply for “conservatism” because the effect on the calculated P_c can be considerable. The best overall strategy for applying conservatism, should one wish that, is to apply it at the end of the process by lowering the P_c threshold at which mitigation actions should occur. Injecting conservatism into different places throughout the P_c calculation makes it difficult to determine how much conservatism has actually been introduced, whereas addressing this desire through a modification of the P_c threshold for mitigation allows it to be understood precisely.

Mashiku and Hejduk (2019) recently completed a study of different hard-body radius calculation and setting strategies, and a streamlined summary of the possibilities examined is provided below:

1. **Large *a priori* value.** For some years it was standard practice simply to choose a hard-body radius value that was notably larger than the expected actual size of the combined primary and secondary object; 20 meters is a value that was typically used. Perhaps in the early days of conjunction assessment, this was an acceptable initial screening strategy to identify potential serious events, and the hard-body radius would then be reduced when analysis began in earnest. As the space catalog has grown in size, and especially with the recent growth through the deployment of the Space Fence radar, this particular strategy merely creates additional false alarms that needlessly burden the process. Nearly all O/Os have moved away from this hard-body radius strategy.
2. **Circumscribing sphere.** The use of a circumscribing sphere to set the primary object’s hard-body radius is perhaps the most commonly used present operational technique, which admits of two typical variants: placing the sphere’s center at the center of mass of the primary satellite and defining the radius by the length from this center to the satellite’s most distant extremity; or allowing the center point to float freely and then defining the smallest circumscribing sphere. The overall sphere size then has to be increased by the expected size of the secondary object using either an averaged value or an estimate for the particular secondary encountered. This size could be obtained either from known or published dimensions (for intact spacecraft or rocket bodies) or estimated from remote sensing data, such as radar cross-section or photometric brightness measurements. In the latter case, the estimated hard-body radius size of the secondary may also have an associated uncertainty estimate, which can also be incorporated into the P_c estimation process (as discussed in more detail below).
3. **Maximum projected area into any plane.** Since the circumscribing sphere described above most often ends up being projected into the conjunction plane, it is instructive to examine in more detail the implications of such a projection. Clearly the sphere itself will project as a circle, but the projection of the three-dimensional spacecraft inside will necessarily be smaller in area than the projected circle, and for some spacecraft shapes and orientations, it will be substantially smaller in area. In this latter case, the substantial “white space” within the projected circular area not occupied by the primary could justifiably be excluded in the P_c estimation process, especially for the most common



debris-encounter scenario when the incoming secondary object is much smaller than the primary asset. A straightforward way to address this issue that does require knowledge of the satellite's actual orientation in relation to the conjunction plane is simply to determine in advance the maximum area that the satellite can possibly project into any plane (based on a three-dimensional CAD¹⁸ model of the satellite) and use a hard-body radius circle of that equivalent area (which of course must then be enlarged to include the estimated size of the secondary) for P_c estimation. It is true that this is a conservative formulation in that it uses the maximum possible projected area, but this is often substantially smaller than the area of the projected circumscribing sphere. One could argue that uncertainty is introduced by using the equivalent circular area rather than a contour integral to perform the integration over the actual projected shape, but individual exploratory examples show that this difference is usually negligibly small, and in any case, the most conservative projection approach should compensate for any differences in the shape chosen to represent the hard-body radius area for the P_c calculation.

4. **Projection into actual conjunction plane.** The most accurate, and at the same time the most difficult, approach is to perform a projection of the primary satellite's shape into the actual conjunction plane. Specifically, this requires a three-dimensional CAD model of the satellite plus knowledge of its inertial attitude and the orientation of any major articulating components at TCA along with a calculation to project the resulting shape into the conjunction plane. Once this projection is obtained, its boundaries have to be augmented to account for the expected size of the secondary, and the integration of the joint covariance probability density can take place over this figure via contour integration or over a more convenient shape of equivalent area. Chan (2019) recently proposed a method to decompose complex shapes into individual triangles and use an equivalent-area method to evaluate the P_c for each triangle; the composite P_c is simply the sum of the P_c values for these individual trials of decomposition.

Each successive approach among the four presented brings greater precision to the hard-body radius determination but at the same time, additional complexity. A reasonable *via media* would appear to be approach 3) above, which keeps the hard-body radius value grounded in reality and free from excessive conservatism but avoids the difficulties of gathering and maintaining shape and attitude data to enable a detailed projection calculation for each conjunction.

To facilitate P_c estimation, CARA has undertaken an effort to estimate hard-body radii of unknown orbiting objects based on radar cross section (RCS) measurements obtained by the Space Fence radar system (Baars and Hall 2022; Hall and Baars 2022). Even after accounting for radar calibration irregularities and occasional outlier data points, such RCS measurements have considerable point-to-point scatter, and the process of converting the RCS data into hard-body radius estimates introduces considerable additional uncertainty. The resulting hard-body radius uncertainty PDFs are non-Gaussian, although they can be roughly approximated using a log-normal distribution. Notably, RCS-based hard-body radius estimates are typically uncertain by factors of two to three, so it is essential that P_c estimates account for these uncertainties. For an

¹⁸ Computer-aided Design



unknown secondary involved in a conjunction, the RCS-based uncertainty PDF can be used to calculate a mean hard-body radius estimate, \bar{R}_2 , and an associated variance, $\sigma_{R_2}^2$. As mentioned previously, for many conjunctions, the estimated P_c value varies roughly in proportion to the square of the hard-body radius. In these cases, the appropriate hard-body radius to use for P_c estimation is given by the effective combined hard-body radius

$$R_{\text{eff}} = \sqrt{(R_1 + \bar{R}_2)^2 + \sigma_{R_2}^2} \quad (\text{N-17})$$

with R_1 representing the primary object's hard-body radius, usually established using methods 2 or 3 listed above, as discussed previously. (The current recommendation for the less often used method 4 is to increase the projected shape of the primary object outwardly on the conjunction plane by the length $\bar{R}_2 + 3\sigma_{R_2}$ to produce a conservative P_c estimate, although CARA continues to research a more accurate approach in these cases.) So for most cases, CARA recommends calculating P_c values using the combined hard-body radius given in equation (N-17) for all conjunctions involving secondary objects with uncertain sizes, partly because of the formula's relative simplicity, but primarily because using the effective radius approach reproduces remarkably well the more accurate RCS-based P_c estimates calculated using Monte Carlo analyses. (See Hall and Baars 2022 for details.)

Currently, Space Fence RCS measurements sufficient for size estimation are available for over 90% of CARA conjunctions involving unknown secondary objects (Baars and Hall 2022). Analysis indicates that about 98% of such conjunctions involve secondary objects with mean hard-body radius estimates less than 35 cm, and only about 0.3% have $\bar{R}_2 > 1.5$ m. For known objects (e.g., active or retired payloads, rocket-bodies), this approach tabulates the known hard-body radii with zero uncertainty, along with a reference for the source of the size information. For unknown objects with sufficient RCS data (which includes a large fraction of tracked LEO orbital debris objects), this approach tabulates the mean estimated hard-body radius and the 1-sigma uncertainty, which can be used in equation (N-17). For reference, this approach also tabulates the median hard body radius values, as well as the associated 95% and 99% confidence intervals, as estimated from the actual RCS-based uncertainty PDF. For unknown objects with insufficient RCS data, one can assign a reasonably conservative default size estimate of 1.5 m.